OPTIMISATION AND NONLINEAR DYNAMICS OF FED BATCH BIOCHEMIAL REACTOR

A Thesis Submitted

in Partial Fulfillment of the Requirements

for the Degree of

Master of Technology

by

Alok Jayant

to the

DEPARTMENT OF CHEMICAL ENGINEERING

INDIAN INSTITUTE OF TECHNOLOGY, KANPUR

December, 1996

CERTIFICATE

Certified that the work contained in this thesis entitled, "Optimisation and Nonlinear Dynamics of Fed Fatch Biochemial Reactor", by Alok Jayant has been carried out under my supervision and that this work has not been submitted elsewhere for a degree.

(Dr. S. Pushpavanam)
Department of Chemical Engineering
Indian Institute of Technology
Kanpur

December, 1996

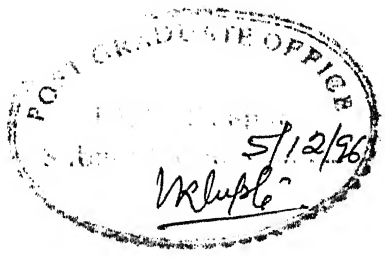

ACKNOWLEDGEMENT

I am deeply grateful to my thesis supervisor, Dr. S. Pushpavanam for encouragement, support and helping nature. It was a great pleasure working under him.

I am thankful to my labmates Rahul, Bhadri, Joydeb, Pande Ji, Murthy, Imran, Samir and Vikas for their warmth and understanding.

I am very thankful to my friends, Jhumma, Phalguni, Prashant, Prasoon, Sanjay, Srinivas, Narayanan, Shishir, Shamim, Hall-IV (Top G) and Vivek Awasthi for keeping my moral high throughout this work.

Alok Jayant

CONTENTS

List of Figures

Fig. 3.3: Plot of X vs. time for a rapid fill RFB for r = 0.7.

Fig. 3.4: Bifurcation diagram of a repeated fed-batch, constant $\bar{F}$ when $S_F < S^*$, $S_F = 5$, $r = 0.7$.

Fig. 3.5: Bifurcation diagram of a repeated fed-batch, constant $\bar{F}$ when $S_F > S^*$, $S_F = 25$, $r = 0.3$.

Fig. 3.6: Optimal flow rate profile (fixed final volume, fixed final time). Effect of parameter ρ for a repeated fed-batch biochemical reactor when $S_F < S^*$ (see Table 3.1).

Fig. 3.7: Plot of X vs. time for $\rho = 1.0$ for optimal profile of Fig. 3.6.

Fig. 3.8: Plot of flow-rate profile of a fixed final volume, fixed final time for $\rho = 4.0$ when $S_F > S^*$, $r = 0.7$, $S_F = 14.75$.

Fig. 3.9: Plot of X vs. time of a fixed final volume, fixed final time for $\rho = 4.0$ when $S_F > S^*$, $r = 0.7$, $S_F = 14.75$.

Fig. 3.10: Optimal flow rate profile (free final volume, fixed final time). Effect of parameter ρ for a repeated fed-batch biochemical reactor when $S_F < S^*$ (see Table 3.2).

Fig. 4.1 : Bifurcation diagram of a repeated fed batch, constant $\bar{F}$ when $S_F = 25.0$, $r = 0.7$.

Fig. 4.2 Plot of X versus cycle time for Kc=0.2

Fig. 4.3 Plot of constant flow rate $\bar{F}$ in each cycle to obtain the set-point X_{sp}= 8.606 for Kc = 0.2.

Fig. 4.4 Plot of X versus cycle time for Kc = 0.5

Fig. 4.5 Plot of constant flow rate $\bar{F}$ in each cycle to obtain the set-point X_{sp}= 8.606 for Kc = 0.5.

Nomenclature

D	:	Dilution rate (hr^{-1})
F	:	Flow rate (l/hr)
F_{max}	:	maximum flow rate
F_{min}	:	minimum flow rate
H	:	Hamiltonian
S_o	:	initial substrate concentration (g/l)
S_F	:	feed substrate concentration (g/l)
t_o	:	initial time
t_f	:	final time
V_o	:	initial volume
V_f	:	final volume
X_o	:	initial biomass concentration
X_f	:	final biomass concentration
Y	:	yield of the reaction

Greek

μ	:	kinetic expression
μ_{max}	:	maximum specific growth rate hr^{-1}
α, β, γ	:	parametric constants in the kinetic expression
λ_x, λ_v	:	adjoint variables in X,V
ρ	:	weightage of cost factor

Subscripts

f	:	final
o	:	initial
max	:	maximum
min	:	minimum
F	:	feed
*	:	dimensionless

Superscripts

+	:	just after feed
-	:	just before feed

CHAPTER 1

1.1 Introduction

Microbial biochemical reactions in absence of air are calle fermentation reactions. These reactions are generally anaerobi in nature. The examples of fermentation include the industrial scale manufacture of glutamate, lysine, threonine, valine, glutamine, aspartic acid, anthranine and other amino acids.

Three major challanges associated with such systems involves modelling, optimisation and control. The challenges involved in modelling is to come up with suitable models to predict the experimental data. However modelling is not trivial as most reactions have unknown kinetics. Emperical relationship such as Monod, Blackman hole model, Heldane have been used from time to time to predict the experimental behaviour such as decay of substrate with time, growth of cell with time etc.

Optimisation problems are associated with maximising the cell concentration or the product formation along with the substrate or product inhibition. Various feeding stratagey have been used to find the optimum of the same. Nonlinear programming techniques like SQP or Pontrayagin's Maximum principle are used to solved such problems.

In the second chapter of this work we optimise the system performance of a non-repeated fed batch biochemical reactor using the Pontrayagin's Maximum principle for maximising the biomass concentration using a nonlinear objective function without the constraints on the flow rate profile for the following cases.

(1) Fixed final volume, fixed final time, (2) Free final volume, fixed final time, (3) Free final volume, fixed final volume, (4) Free final volume, free final time.

In the third chapter of this work we study the possible bifurcations diagrams of a CSTR, rapid fill repeated fed betch reactor and a repeated fed batch biochemical reactor filled with constant $\bar{F}$. We also optimise the system performance for maximising the biomass concentration for the following two cases. (1) Fixed final volume, fixed final time, (2) Free final volume, fixed final time.

In the fourth chapter of my thesis we discuss the proportional control of a repeated fed- batch reactor around a desired but unstable periodic state .The control action is based on measuring the biomass concentration at the end of the cycle.

CHAPTER 2

Optimisation of Non-repeated Fed-Batch Biochemical Reactors

2.1 Introduction

Biochemical fermentation reactions are frequently characterised by substrate inhibition and/or product inhibition. The performance of these reactors is optimal when operated in the fed batch mode. Here the substrate is added to the reactor during the course of the reaction. The biomass is usually present initially in the reactor. The control variable is the substrate feed rate.

The optimal performance of fermentation reactors in the fed batch mode has been investigated with the objective of minimising either 1) the biomass production or (ii) the product formed[4,5]. Two classical methods that have been used to study the problem are (i) Pontryagin's continuous maximum principle and (ii) nonlinear optimisation techniques as SQP[5,6]. The model system most extensively investigated is characterised by a single reaction. The reaction rate varies linearly with biomass and is assumed to have a Haldane dependency on the substrate.

Weigand[15] considered the problem of maximising cell production in a repeated fed batch mode of operation. He obtained an analytical expression relating the total reaction time with biomass concentration under the optimal conditions. In his analysis however he did not assume an upper bound on the permissible flow rate.

Bonte et al.[2] and Modak[11] determined the optimal feeding

profiles for different kinetic models. They developed a computational scheme to obtain the feeding policy which maximised a) pencillin production and b) cell mass production.

The optimal control problem considered in these works is linear in the control variable, the substrate feed rate. It is hence singular in nature. The optimal policy consists of different portions i) when the feed rate is held at its minimum ii) when the feed rate is held at its maximum and iii) when the feed rate follows a singular arc (Cazzador)[4]. The numerical computation of the optimal profile however, needs a physical insight into the problem. This is necessary to determine the exact sequence of the different portions which constitute the optimal profile (Modak)[11].

In a non-biochemical engineering context optimal feed rate policies were obtained using pulse feeds at discrete intervals of time by Levin[8]. Sequential Quadratic Programming was used by Beigler[1], Morrison and Sargent[10] and Vaisliadis et al.[14]

Shukla et al.[13] used a sequential quadratic programming technique to obtain the optimum feed rate profile. They divided the entire interval of operation into different segments. The feed rate in each interval was assumed to be a constant. The optimal feed rate policy thus determined does not use any information from the physics. This approach provides a general mathematical basis for obtaining the optimal solution. It is useful when the interactions between the different variables is complex. The disadvantage of this technique lies in the fact that it is computationaly intensive.

In this work we propose an alternative method to investigate the singular optimisation problem discussed. The objective function is modified to include a term which is representative of the cost involved in prefering the optimal policy over the average constant flow rate. This is quadratic in the control variable. The problem is now nonsingular and can be analysed elegantly using the maximum principle. The classical singular problem investigated can be obtained as a limiting case of a nonsingular problem, by reducing the weightage assigned to the quadratic term. This technique can be used to provide us insight into the different regimes of the control variable and the sequence in which they occur. This information can then be used to solve the classical problem using the computational technique presented in Modak[11].

In this work we analyse the non-repeated fed batch mode of operation. We analyse four cases of reactor operation (1) fixed final time, fixed final volume (2) fixed final time, free final volume (3) free final time, fixed final volume (4) free final time, free final volume. We also discuss the effect of different initial conditions on the optimal control profiles. Throughout this study we assume that there are no bounds on the flow rates.

2.2 Mathematical model

The evolution equations which describe the reactor performance are:

$$\dot{(VX)} = \mu(S)XV \qquad 2.1(a)$$

$$\dot{(VS)} = \frac{-\mu(S)XV}{Y} + FS_F \qquad 2.1(b)$$

$$\dot{(V)} = F \qquad 2.1(c)$$

Here $\mu(S)$ represents the reaction rate dependency on the substrate concentration S, Y is the constant yield, S_F is the substrate concentration in the feed, F is the flow rate of the substrate.

Here we assume

$$\mu(S) = \frac{\mu_{max} S}{\alpha S^2 + \beta S + \gamma}$$

From equations (2.1a-c) it follows that

$$\left(\frac{(\dot{XV})}{Y} + (\dot{SV}) - (\dot{VS_F}) \right) = 0 \qquad 2.2(a)$$

We now obtain

$$S = S_F + \frac{V_o}{V} \left(\frac{X_o}{Y} + S_o - S_F \right) - \frac{X}{Y} = g(X,V) \qquad 2.2(b)$$

Here the subscript 'o' is used to indicate the initial conditions in the reactor.

This relationship is valid for all time and can be used to relate S(t) to X(t). It can be used to eliminate 'S' in the equations 2.1(a-c). Substituting in 2.1(a-c), we can reduce the three dimensional system to the following two dimensional system.

$$\dot{X} = X\mu(g(X,V) - \frac{FX}{V} \qquad 2.3(a)$$

$$\dot{V} = F \qquad 2.3(b)$$

Our objective is to determine the feed-rate profile F(t) which maximises the biomass productivity at the terminal state. This gives rise to the objective function.

$$\underset{F(t)}{\text{Minimize}} \quad J = -X_f V_f \qquad 2.4(a)$$

This problem however, is singular since the control variable 'F' occurs linearly in 2.3(a,b). In this work we modify the objective function as

$$\underset{F(t)}{\text{Minimize}} \quad J = -X_f V_f + \rho \int_o^{t_f} (F-\bar{F})^2 \, dt \qquad 2.4(b)$$

The subscript 'f' is used to denote the final state of the system. The introduction of the quadratic term in 2.4(b) renders the problem non-singular. It can be interpreted as being representative of the cost involved in maintaining the optimal profile F(t) instead of the average profile $\bar{F}$. It is hence proportional to the deviation $(F - \bar{F})^2$. The scalar ρ is a weightage factor which can be used to change the importance of the two terms.

The optimal control problem can be solved elegantly by using Pontryagin's Maximum Principle. We define the Hamiltonian

$$H = \lambda_x \left[X\mu(g(X,V)) - \frac{FX}{V}\right] + \lambda_v F + \rho \, (F-\bar{F})^2 \qquad (2.5)$$

Here λ_x and λ_v are the adjoint variables associated with 2.3(a,b). Their evolution is governed by

$$\dot{\lambda}_x = -\lambda_x \left[\mu(g(X,V) + X \frac{\partial \mu(g(X,V))}{\partial X} - \frac{F}{V}\right] \qquad 2.6(a)$$

$$\dot{\lambda}_v = -\lambda_x \left[X \frac{\partial \mu(g(X,V))}{\partial V} + \frac{FX}{V^2}\right] \qquad 2.6(b)$$

The optimal flow rate profile is obtained by setting

$$\dot{H}_F = 0$$

This gives

$$F = \bar{F} + \frac{1}{2\rho} \left(\lambda_x \frac{X}{V} - \lambda_v\right) \qquad (2.7)$$

In this work we analyse the optimum profile for the four different cases mentioned earlier . For each of the cases the equations 2.3(a,b), 2.4b, 2.6(a,b) have to be solved such that they satisfy certain conditions.

Case I: Fixed final volume, fixed final time - The optimum profile is obtained when the following conditions are satisfied.

$$\lambda_x\ (t_f) + V_f = 0$$

$$\text{or} \qquad \mathbf{F}_I = 0$$

$$V\ (t_f) - V_f = 0 \tag{2.8}$$

Case II: Fixed final time, free final volume - The optimum profile now satisfies

$$\lambda_x\ (t_f) + V(t_f) = 0$$

$$\text{or} \qquad \mathbf{F}_{II} = 0$$

$$\lambda_v\ (t_f) + X(t_f) = 0 \tag{2.9}$$

Case III: Fixed final volume, free final time - Here the optimal profile must satisfy

$$\lambda_x\ (t_f) + V_f = 0$$

$$V\ (t_f) - V_f = 0 \qquad \text{or} \qquad \mathbf{F}_{III} = 0$$

$$H\ (t_f) = 0 \tag{2.10}$$

Case IV: Free final volume free final time - Here the optimum profile must satisfy

$$\lambda_x\ (t_f) + V(t_f) = 0$$

$$\lambda_v\ (t_f) + X(t_f) = 0 \qquad \text{or} \qquad \mathbf{F}_{IV} = 0$$

$$H\ (t_f) = 0 \tag{2.11}$$

The optimal profile is obtained for each case when the respective conditions are satisfied. The optimisation problem is a two-point boundary value problem, since the conditions on X,V are defined at t=0, while those on the adjoint variables have to be satisfied at $t = t_f$.

The solution hence has to be obtained iteratively using a technique like the Newton Raphson method. Thus for cases I, II we iterate on variables λ_{xo}, λ_{vo} while for cases III, IV we iterate on λ_{xo}, λ_{vo}, t_f.

The iterative scheme is

$$U_i^{n+1} = U_i^n - J_i^{-1} \mathbf{F}_i$$

where

$$U_I = U_{II} = [\lambda_{xo}, \quad \lambda_{vo}]^t$$

$$U_{III} = U_{IV} = [\lambda_{xo}, \quad \lambda_{vo}, \; t_f]^t$$

$$J_I = \begin{bmatrix} \frac{\partial \lambda_x}{\partial \lambda_{xo}} & \frac{\partial \lambda_x}{\partial \lambda_{vo}} \\ \frac{\partial V}{\partial \lambda_{xo}} & \frac{\partial V}{\partial \lambda_{vo}} \end{bmatrix}^{-1} \qquad (2.12)$$

$$J_{II} = \begin{bmatrix} \frac{\partial \lambda_x}{\partial \lambda_{xo}} + \frac{\partial V}{\partial \lambda_{xo}} & \frac{\partial \lambda_x}{\partial \lambda_{vo}} + \frac{\partial V}{\partial \lambda_{vo}} \\ \frac{\partial \lambda_v}{\partial \lambda_{xo}} + \frac{\partial X}{\partial \lambda_{xo}} & \frac{\partial \lambda_v}{\partial \lambda_{vo}} + \frac{\partial X}{\partial \lambda_{vo}} \end{bmatrix}^{-1} \qquad (2.13)$$

$$J_{III} = \begin{bmatrix} \frac{\partial \lambda_x}{\partial \lambda_{xo}} & \frac{\partial \lambda_x}{\partial \lambda_{vo}} & \frac{\partial \lambda_x}{\partial t} \\ \frac{\partial V}{\partial \lambda_{xo}} & \frac{\partial V}{\partial \lambda_{vo}} & \frac{\partial V}{\partial t} \\ \frac{\partial H}{\partial \lambda_{xo}} & \frac{\partial H}{\partial \lambda_{vo}} & \frac{\partial H}{\partial t} \end{bmatrix}^{-1} \qquad (2.14)$$

$$J_{IV} = \begin{bmatrix} \frac{\partial \lambda_x}{\partial \lambda_{xo}} + \frac{\partial V}{\partial \lambda_{xo}} & \frac{\partial \lambda_x}{\partial \lambda_{vo}} + \frac{\partial V}{\partial \lambda_{vo}} & \frac{\partial \lambda_x}{\partial t} + \frac{\partial V}{\partial t} \\ \frac{\partial \lambda_v}{\partial \lambda_{xo}} + \frac{\partial X}{\partial \lambda_{xo}} & \frac{\partial \lambda_v}{\partial \lambda_{vo}} + \frac{\partial X}{\partial \lambda_{vo}} & \frac{\partial \lambda_v}{\partial t} + \frac{\partial X}{\partial t} \\ \frac{\partial H}{\partial \lambda_{xo}} & \frac{\partial H}{\partial \lambda_{vo}} & \frac{\partial H}{\partial t} \end{bmatrix}^{-1} \qquad (2.15)$$

In the above scheme the elements of the Jacobian matrix have to be evaluated at the terminal stage i.e. final time. The solution technique hence relies on the accurate evaluation of these derivatives. The equations which govern the evolution of these derivatives are given in Appendix I & II.

2.3 Results and Discussion

The method of solution discussed above was used to obtain the performance of the fed batch reactor for all the four cases. The kinetic parameter chosen for all the computations reported in this work are $\mu_{max} = 5.2\ hr^{-1}$, $\alpha = 1.0$, $\beta = 25.0$, $\gamma = 62.9$.

The other parameters chosen for optimisation are $V_o = 7.0$ l, $S_o = 0.143\ 10^{-3}$ g/l, $X_o = 0.1$, $S_f = 500$, $V_f = 10$ l, $t_f = 10$ hr, $\rho = 4.0$ for case I. The corresponding optimal flow rate profile is shown in Fig. 2.1. The biomass ($X_f V_f$) at the end of cycle is 1.2430. The biomass obtained when the substrate is added at an average flow rate $\bar{F} = 0.3$ is $X_f V_f = 1.2259$. The biomass while operated in the batch mode i.e., all the substrate is added initially to the reactor is 0.9416. For this case I, there is an improvement of 1.375% and 24.25% respectively over fed batch operation with a constant flow rate and batch operation.

The effect of the parameter ρ on the optimal feed rate policy is depicted in Fig. 2.2. For high values of ρ, the deviation from the average flow rate has to be minimised and so the optimal flow rate profile is as close to $\bar{F}$ as possible. This yields $X_f V_f = 1.2430$. When we decrease the parameter 'ρ' the optimal profile exhibits a significant deviation from $\bar{F}$. Now the weightage of the cost effect of the deviation from $\bar{F}$ has been decreased. So the optimal flow rate profile can deviate from $\bar{F}$ and there is a substantial improvement in the total amount of biomass produced (For $\rho = 0.8$, $X_f V_f = 1.4081$).

The results for the other four cases of operation are summarised in Table 2.1. In this table we have used the same

weighting factor 'ρ' for all four cases. The improvement in biomass produced for case IV is 50.76% and 15.31% over batch and a fed batch operation with a constant flow rate. This is the total optimisation problem, since here we constrain neither the final time nor the final volume. The improvements in reactor performance for cases II, III where we constrain either the final time or the final volume lie in between the case I (where both are constrained) and case IV (with no constraints).

As discussed earlier, the improvement in reactor performance as measured by the amount of biomass produced at the end of the cycle is more pronounced as we decrease ρ. However, as we decrease ρ, the problem becomes singular and the convergence of the numerical scheme is not ensured. The effect of ρ on the optimal performance can be seen by comparing the results presented in Table 2.2 and Table 2.1. As ρ is decreased the total biomass produced at the end of the reactor cycle increases for each case.

The corresponding optimal flow-rate profile for each of these cases is depicted in Fig 2.3(a-d). The values of the parameter 'ρ' for which the simulations were performed are also indicated.

In this mode of operation the optimal profile is dependent on the initial conditions. The kinetic expression is characterised by the substrate concentration S^* at which the reaction rate is a maximum. Two other characteristic quantities quantifying substrate concentration are S_o, the initial concentration and S_f, the feed concentration. Cazzador[4] determined the effect of initial conditions on the optimal flow rate profile. We now discuss this effect for, different orderings of S_o, S^*, S_f.

$S^* < S_F < S_o$ — The optimal flow rate profile for this case is shown in Fig. 2.4a. The flow rate decreases with time. The initial substrate concentration is very large here. The reaction rate at this S_o is low. Starting with a high 'F' we reduce the substrate concentration from S_o to S^*. This increases the reaction rate and results in an optimal performance.

$S^* < S_o < S_F$ — Here the optimal flow rate profile increase with time (Fig. 2.4b). The reaction rate at S_o is lower than the maximum. Addition of substrate at S_F would servee to only increase S and thereby decrease the reaction rate further. The addition of the substrate hence has to be initially low as the addition of high F(t) initially would increase S_o to a value away from S^* thereby lowering the reaction rate.

$S_o < S^* < S_F$ — Here again the flow rate profile decreases with time. The addition of a significant amount of substrate (high S_F) initially increases S_o close to S^* and this increases the reaction rate. As time progresses the flow rate is decreased so as to maintain S_F close S^* (Fig. 2.4c)

$S_o < S^* < S_F$ — Here when S_F is significantly high, the flow rate is initially high. This raises S_o to S^*. The flow-rate is then decreased to prevent S_F from increasing beyond S^* which would decrease the reaction rate. The gradual increase in the flow rate in the second half ensures that the substrate concentration is around S^* (Fig. 2.4d).

$S_F < S^* < S_o$ — Here the initial concentration is high so the reaction rate is low. A significant amount of S_F is added initially thereby reducing S_o to close to S^*. This generates the

decreasing profile of F(t) (Fig. 2.4e).

$S_o < S_F < S^*$ — Here S_o is low and by adding S_F at a high flow rate we increase S_o closer to S^* thereby increasing the reaction rate. The flow rate then decreases with time (Fig. 2.4f).

$S_F < S_o < S^*$ — Here the initial concentration is lower than S^*. The optimal feed rate profile increases with time. Here initial concentration is closer to S^* than S_F. Adding a high amount of fresh feed would only lower S_o and the reaction rate. So it is necessary to start with a low flow rate. The flow rate increases with time and thereby filling up the reactor (Fig. 2.4g).

The quantitative results of a typical set of calculations is tabulated in Table 2.3. Simulations were performed for other cases to study the effect of initial conditions. These also show a similar trend.

In most cases the biomass increases monotonically with time. For some cases there is an increase followed by a decrease and for some there is a decrease followed by an increase, under optimal conditions.A typical variation of the biomass concentration with time is shown in Fig. 2.5.

2.4 Conclusions

In this work we have obtained optimal flow-rate profiles for a singular problem by converting it to a non-singular problem. This is achieved by modifying the objective function.

As we decrease the parameter, ρ, the importance on the variation of F is reduced. Here a more significant variation in F

is permissible and there is a significant improvement in biomass produced. The convergence of the numerical scheme is ensured for large values of ρ. As we lower the parameter ρ however, the optimisation program approaches the singular limit. For low ρ, the optimisation program does not converge easily. The cut off value of ρ, above which convergence occurs depends on the case being studied.

This cut off value is low for case I and high for case IV. This is to be expected as case IV is the compeltely optimal problem. Here are no constraints on V_f or t_f.

The optimal profile generated exhibit a continuous variation in F(t). This is to be expected as now we have a non-singular problem. The optimal profiles generated can be used to obtain qualitative insight into the sequence of control actions of the singular problem. Thus for the case represented in Fig. 2.3a, the optimal profile for the singular problem (with ρ = 0) would consist of a time interval where F(t) is F_{max}, followed by a period where it is F_{min}. This in its turn would then be followed by a singular arc.

The technique proposed in this work can be used to obtain qualitative insight into the diffierent sequences of control actions for the singular problem. The techniques proposed by Modak[11] can then be used to numerically solve the problem elegantly.

CHAPTER 3

On the Bifurcation Features and the Optimal Performance of a Repeated Fed-Batch Reactor

3.1 Introduction

Biochemical reactions are characterised frequently by substrate inhibition. Reactors sustaining such reactions exhibit an optimal performance when operated in a fed-batch mode. Here the substrate is usually added to the reactor over a period of time (Cazzador[4], San and Stephanopolous[12]). These works deal with the performance of non-repeated fed-batch reactors.

The control variable i.e., substrate feed rate occurs linearly in the problem. The optimal control profile is hence bang-bang and/or consists of a singular arc. Weigand[15] has analysed the performance of reactors operated in a repeated fed batch mode. He analytically established that the optimal reactor operation was obtained when the flow rate was first at its upper bound, F_{max}, then followed by a singular arc, and finally a segment when F(t) was at its lower bound, F_{min}, (usually zero).

The non-repeated fed-batch mode of operation is similar to the operation of the batch reactor as the initial conditions influence the system performance. For the repeated fed-batch mode of operation the initial conditions determine the terminal state only when multiple co-existing states exist in the system. Here the terminal state i.e. the system state after a large number of cycles is a periodic state. This is similar to the steady-state of a continuously stirred tank reactor (CSTR).

In many systems however, it is not possible to obtain optimal profiles analytically. The numerical computation of the optimal profile needs insight into the interaction between the different variables. This allows us to determine qualitatively the sequence of control variable profiles, which have to be maintained. A bad choice of the sequence may result in non-convergence of the numerical scheme for problems singular in the control variable (Modak)[11].

In this work we establish that the biomass concentration and the substrate satisfy the stoichiometric relationship in the terminal state of the repeated fed-batch operation. We also discuss how the bifurcation features of the repeated fed-batch reactor when filled instantaneously are similar to that of a CSTR.

We also consider the optimal operation of the repeated fed-batch reactor. The objective function is modified to include the cost associated with preferring the optimal profile over a constant feed-rate. This is assumed to be proportional to the square of the deviation variable. The problem is now rendered non-singular and can be solved elegantly using Pontryagin's maximum principle. We show how decreasing the effect of the weightage on the cost factor, allows us to approach the limit of the classical singular problem. This technique can be used to determine the sequence of i.e., ordering of the control actions for the classical singular problem. This is especially useful in systems where it is not possible to elegantly obtain analytical solutions and the physical interaction of the variables is complex. The numerical technique proposed by Modak[11] can then be

implemented elegantly to compute the quantitative profile for the singular problem.

3.2 Mathematical model

In this work the evolution equations of biomass, X, and substrate concentration, S are assumed to be given by

$$\dot{(XV)} = X\mu(S)V \qquad 3.1(a)$$

$$\dot{(SV)} = -X\frac{\mu(S)V}{Y} + FS_F \qquad 3.1(b)$$

$$\dot{V} = F \qquad 3.1(c)$$

The reactor is operated cyclically over a fixed time t_f. Over this period the volume increases from V_o to V_f i.e.,

$$V(t_o) = V_o \qquad 3.2(a)$$

$$V(t_f) = V_f \qquad 3.2(b)$$

At the end of the cycle the reactor contents are partially removed to reduce V_f to V_o. This reduces the volume of the reactor. The concentration at the beginning and at the end of cycle are however equal. So the terminal state satisfies

$$X(t_o) = X(t_f) \qquad 3.3(a)$$

$$S(t_o) = S(t_f) \qquad 3.3(b)$$

In the repeated fed-batch mode of operation we are not interested in the transient behaviour of the system. This can be obtained from a dynamic simulation. The terminal state i.e., after the initial transients have decayed is of importance. This is a periodic state as the state variables satisfy 3(a,b). This arises due to the periodic forcing imposed by the periodic variation in the substrate feed-rate. This periodic state is analogous to the steady-state behaviour of the CSTR.

3.3 Relationship between, X,S in the terminal state

We now establish that the biomass concentration X, and the substrate concentration S, satisfy the stoichiometric relationship at all instants of time. From the equations (3.1a,c), we obtain

$$\left(\frac{(\dot{XV})}{Y} + (\dot{SV}) - (\dot{VS_F}) \right) = 0 \qquad (3.4)$$

or $$\left(\frac{X(t_o)}{Y} + S(t_o) - S_F \right) V_o = \left(\frac{X(t_f)}{Y} + S(t_f) - S_F \right) V_f \qquad (3.5)$$

This relationship must be satisfied for each cycle. Thus we have, for the ith cycle

$$\left(\frac{X(t_f)}{Y} + S(t_f) - S_F \right)_i = \left(\frac{X(t_o)}{Y} + S(t_o) - S_F \right)_i \frac{V_o}{V_f} \qquad (3.6)$$

Since the concentrations at the end of the ith cycle, are same as the concentrations at the beginning of the $(i+1)^{th}$ cycle, we have

$$\left(\frac{X(t_o)}{Y} + S(t_o) - S_F \right)_{i+1} = \left(\frac{X(t_o)}{Y} + S(t_o) - S_F \right)_i \frac{V_o}{V_f} \qquad 3.7(a)$$

This recursive relationship can be used to obtain

$$\left(\frac{X(t_o)}{Y} + S(t_o) \right)_n = \left(\frac{X(t_o)}{Y} + S(t_o) - S_F \right) \left(\frac{V_o}{V_f} \right)^{n-1} + S_F \qquad 3.7(b)$$

For $n \longrightarrow \infty$, $\left(\frac{V_o}{V_f} \right)^{n-1} \longrightarrow 0$ as $\frac{V_o}{V_f} < 1$ and we have at the terminal state (after a sufficient number of cycles)

$$\left(\frac{X(t_o)}{Y} + S(t_o) \right) = S_F \qquad (3.8)$$

Clearly from this it follows, at every time instant

$$S(t) = S_F - \frac{X(t)}{Y} = g(X) \qquad (3.9)$$

The biomass and substrate satisfy the stoichiometric

relationship (3.9) at all instants of time.

This can be used to reduce the three dimensional system (1a-c) to the two dimensional system

$$\dot{X} = X\mu(g(X)) - \frac{FX}{V} \qquad 3.10(a)$$

$$\dot{V} = F \qquad 3.10(b)$$

The rate dependency on the substrate throughout this work is assumed to be of the Haldane form

$$\mu(S) = \frac{\mu_{max}\, S}{\alpha S^2 + \beta S + \gamma} \qquad (3.11)$$

3.4 The Rapid Fill Case

The repeated fed-batch operation can be carried out by a filling the reactor from V_o to V_f instantaneously at the beginning of every cycle . In this mode the reaction is carried out in a batch mode for t_f. Thus the evolution is governed by

$$\dot{X} = \mu(S_F - \frac{X}{Y})\, X \qquad 3.12(a)$$

However, now the concentration at the beginning of a cycle after the pulse is added i.e. at t_o^+ is different from that at the end of the previous cycle i.e. at t_f^-. From the mass balance we have

$$V_f\, X(t_o^+) = V_o X\, (t_f^-)$$

or

$$X(t_o^+) = r\, X(t_f^-) \qquad 3.12(b)$$

Here, r, represents the draw down ratio V_o/V_f. The biomass concentration now exhibits discontinuities at the end of every period. The dimensionless concentration of biomass $u = (X/YS_F)$ at the end of the cyclic state t_f^- is given by integrating (3.12a)

$$\int_{ru}^{u} \frac{dX}{X\mu\, (S_F - \frac{X}{Y})} = t_f \qquad (3.13)$$

Integrating the expression on the left we have

$$t_f\mu(S_F) = (\alpha S_F^2 + \beta S_F + \gamma)^{-1} \left[\alpha S_F^2(\ln(1/r) - u + ur)\right.$$

$$\left. + \beta S_F \ln(1/r) + \gamma \ln(1/r) - \gamma \ln\left(\frac{1-u}{1-ru}\right)\right] \qquad (3.14)$$

3.5 Formulation of Optimal Control Problem

Our objective in the study of the optimal control problem is to

$$\underset{F(t)}{\text{Minimize}} \quad J = -X_f(t_f)(V(t_f) - V_o) + \rho \int_o^{t_f} (F(t)-\bar{F})^2 \, dt \qquad (3.15)$$

The first term of the right hand side is representative of the increase of the total biomass in the reactor over a cycle while the second represents the cost in preferring the optimal profile over the average F.

The optimal control problem is solved elegantly by using Pontryagin's continuous maximum principle. A detailed discussion of this can be found in Bryson and Ho[3]. The introduction of the quadratic term renders the problem non-singular. We construct the Hamiltonian

$$H = \lambda_x \left[X\mu(g(X)) - \frac{FX}{V}\right] + \lambda_v F + \rho (F-\bar{F})^2 \qquad (3.16)$$

Here the evolution of the adjoint variables λ_x, λ_v is governed by

$$\dot{\lambda}_x = -\lambda_x \left[\mu(g(X)) + X \frac{\partial \mu(g(X))}{\partial X} - \frac{F}{V}\right] \qquad 3.17(a)$$

$$\dot{\lambda}_v = -\lambda_x \left[\frac{FX}{V^2}\right] \qquad 3.17(b)$$

The optimal profile F(t) is obtained by setting $H_F = 0$. This yields

$$F = \bar{F} + \frac{1}{2\rho}\left(\lambda_x \frac{X}{V} - \lambda_v\right) \qquad (3.18)$$

In this work we study two cases of repeated fed-batch operation (I) fixed final volume, fixed final time (II) free final volume, fixed final time. In the latter mode we optimise reactor performance with respect to the draw-down ratio as well.

Each of the above problems is a two point boundary-value problem as some of the variables are specified at t_o, and others at t_f. This has to be solved using an iterative scheme like the shooting method. The three variables to be determined are [λ_{xo}, λ_{vo}, $X(t_o)$]. These are represented vectorically as w. The iterative scheme for the ith case is given by

$$w_i^{n+1} = w_i^n - J_i^{-1} F_i \qquad (3.19)$$

where

<u>for Case I</u>

$$\begin{aligned} &\lambda_x(t_f) + (V_f - V_o) = 0 \\ &V(t_f) - (V_f) = 0 \qquad\qquad F_I = 0 \\ &X(t_f) - X(t_o) = 0 \end{aligned} \qquad 3.20(a)$$

$$J_I = \begin{bmatrix} \frac{\partial \lambda_x}{\partial \lambda_{xo}} & \frac{\partial \lambda_x}{\partial \lambda_{vo}} & \frac{\partial \lambda_x}{\partial X_o} \\ \frac{\partial V}{\partial \lambda_{xo}} & \frac{\partial V}{\partial \lambda_{vo}} & \frac{\partial V}{\partial X_o} \\ \frac{\partial X}{\partial \lambda_{xo}} & \frac{\partial X}{\partial \lambda_{vo}} & \frac{\partial X}{\partial X_o} \end{bmatrix}^{-1} \qquad 3.20(b)$$

<u>and for Case II</u>

$$\begin{aligned} &\lambda_x(t_f) + (V(t_f) - V_o) = 0 \\ &\lambda_v(t_f) + X(t_f) = 0 \qquad\qquad F_{II} = 0 \\ &X(t_f) - X(t_o) = 0 \end{aligned} \qquad (3.21)$$

$$J_{II} = \begin{bmatrix} \frac{\partial \lambda_x}{\partial \lambda_{xo}} + \frac{\partial V}{\partial \lambda_{xo}} & \frac{\partial \lambda_x}{\partial \lambda_{vo}} + \frac{\partial V}{\partial \lambda_{vo}} & \frac{\partial \lambda_x}{\partial X_o} + \frac{\partial V}{\partial X_o} \\ \frac{\partial \lambda_v}{\partial \lambda_{xo}} + \frac{\partial X}{\partial \lambda_{xo}} & \frac{\partial \lambda_v}{\partial \lambda_{vo}} + \frac{\partial X}{\partial \lambda_{vo}} & \frac{\partial \lambda_v}{\partial X_o} + \frac{\partial X}{\partial X_o} \\ \frac{\partial X}{\partial \lambda_{xo}} & \frac{\partial X}{\partial \lambda_{vo}} & \frac{\partial X}{\partial X_o} - 1 \end{bmatrix}^{-1} \tag{3.22}$$

3.6 Results and Discussion

The repeated fed-batch operation of a reactor is the periodically forced operation of a reactor. Here a substrate feed rate profile is maintained over a cycle. The reaction is partially emptied from the final volume to the initial volume at the end of the cycle and the operation is repeated. The biomass and substrate hence exhibits a periodic behaviour with time. This periodic forcing renders the system non-autonomous. This is not immediately obvious from the equations (3.1a-c) whose right hand side are not dependent explicitly on time.

The repeated fed-batch is a periodically forced operation of a batch reactor. This mode of operation is similar to the continuous operation of a CSTR. In the CSTR the basic state of operation is the steady-state. Here the dependent variables X, S are independent of time. The concentrations in the fed batch reactor however, vary cyclically. In particular the concentration at the end of a cycle is identical to that at the beginning provided the flow-rate F(t) is finite for all times (see 3.3(a,b), 3.12(b)).

A possible mode of operation of the repeated fed-batch

reactor as discussed earlier is when the substrate is added instantaneously to the reactor at the beginning of the cycle. The reaction is then allowed to proceed in the batch mode. In this mode of operation the concentration of dimensionless biomass, $X^*(X/YS_F)$ at the end of the cycle is given by the roots u of equation (3.14). In Fig. 3.1a,b we depict the variation of X^* on dimensionless dilution rate D^*. This latter quantity is defined for the fed-batch reactor as $(1-r)/(t_f\ \mu(S_F))$. This figure is called the bifurcation diagram of the system. The dependence of X^* on D^* of the fed-batch reactor is compared with that of the CSTR. Fig. 3.1a exhibits the variation for $S^* > S_F$, and Fig. 3.1b for $S^* < S_F$. Here S^* represents the substrate concentration at which $\frac{d}{dS}\ \mu(S) = 0$, i.e. the rate is a maximum. Throughout this work we have assumed the kinetic parameters to be $\mu_{max} = 5.2$, $\alpha = 1.0$, $\beta = 25.0$, $\gamma = 62.9$. For this choice $S^* = \sqrt{\gamma/\alpha} = 7.9$.

The bifurcation diagram for the CSTR is obtained by the solution to

$$D^* = \mu(S_F(1-X^*))/\mu(S_F) \qquad (3.23)$$

The bifurcation diagram is characterised by a region where bending back occurs for $S^* < S_F$ for fed-batch mode of reactor operation. This is well established for the CSTR (Bailey and Ollis). For the fed-batch operation the condition for the bifurcation diagram to bend back is obtained by setting $\frac{dt_f}{du} = 0$ in (3.14).

In order for the bifurcation diagram to possess a nose i.e. to turn back we further set u=0 and solve for S_F. This yields the relation

$$\frac{(r-1)}{(\alpha S_F^2 + \beta S_F + \gamma)} [\alpha S_F^2 - \gamma] = 0 \qquad (3.24)$$

From this we obtain $S_F = S^* = \sqrt{\gamma/\alpha}$, for the bifurcation diagram to just start bending back. Thus the same criterion on S_F distinguishes the two bifurcation diagrams for the fed-batch reactor as for the CSTR.

It is tempting to interpret the equation (3.13) as predicting wash out to occur at an infinite dilution rate. Clearly the bifurcation diagrams (Fig. 3.1) indicates washout beyond a finite dilution rate. This indicates that the trivial state (of washout) occurs for all dilution rate. This can be seen by examining that the trivial state with $X(t_o^+) = 0$ satisfies the ordinary differential equation and associated boundary conditions (3.1a-c, 3.12a-b) for all t_f's.

The point at which the non-trivial branch emerges from the trivial branch can be obtained by investigating the linear-stability of the basic "wash out" periodic state. This can be done using Floquet theory (Ince)[6]. The stability of the trivial steady-state is obtained by studying the evolution of $\frac{\partial X}{\partial X(t_o)}$. This is governed for the rapid fill case by

$$\frac{d}{dt}\left(\frac{\partial X}{\partial X_o}\right) = \left(\mu(g(X)) + X\frac{\partial \mu(g(X))}{\partial X}\right)\frac{\partial X}{\partial X_o}, \qquad 3.25(a)$$

$$\text{subject to } \left(\frac{\partial X}{\partial X_o}\right)(t_o^+) = 1 \qquad 3.25(b)$$

$$\text{where } \left(\frac{\partial X}{\partial X_o}\right)_{t=t_f^+} = r\left(\frac{\partial X}{\partial X_o}\right)_{t=t_f^-} \qquad 3.25(c)$$

At the wash out state we have $X = 0$. This yields

$$\left(\frac{\partial \dot{X}}{\partial X_o}\right) = \mu(S_F)\ \frac{\partial \dot{X}}{\partial X_o} \qquad 3.26(a)$$

with $$\left(\frac{\partial \dot{X}}{\partial X_o}\right)_{t=t_o^+} = 1 \qquad 3.26(b)$$

Solving this we obtain

$$\left(\frac{\partial X}{\partial X_o}\right)_{t=t_f^+} = r\, e^{\mu(S_F)t_f} \qquad 3.26(c)$$

The washout state is stable when the Floquet multiplier lies within the unit circle, i.e.

$\left|\left(\frac{\partial X}{\partial X_o}\right)_{t=t_f^+}\right| < 1$. This yields $r\, e^{\mu(S_F)t_f} < 1$. In terms of the dimensionless dilution rate, $D^* = \left(\frac{V_f - V_o}{V_f t_f \mu(S_F)}\right) = \left(\frac{(1-r)}{t_f \mu(S_F)}\right)$. The stability condition yields $D^*_{cr} = (r-1)/\ln(r)$. This critical dilution rate is always less than 1 for $0 < r < 1$. Hence wash out occurs earlier in the repeated fed-batch mode than in the CSTR.

For the case $S_F > S^*$, it must be emphasised that the portion of the curve in the positive slope region is unstable in Fig. 3.1. In the mode of rapid fill operation of the repeated fed-batch the biomass concentrations are discontinuous at the beginning of each cycle (Fig. 3.2).We have depicted the variation of the biomass with time in Fig. 3.3 for this case.

In Figure 3.4, 3.5 we have depicted the bifurcation diagrams for the repeated fed-batch mode of operation when the flow-rate is a constant, $\bar{F}$, over the entire cycle. In this diagram the draw-down ratio is a constant. Consequently as we change t_f, to ensure a constant V_o/V_f, we change the average value of $\bar{F}$, to generate the diagrams.

Once again the trivial solution exists for all 't_f' as discussed earlier. The bifurcation of the non-trivial solution from the trivial state occurs where the trivial solution loses its stability. This can be found from Floquet theory by integrating

$$\left(\frac{\partial \dot{X}}{\partial X_o}\right) = \left(\mu(X) + X\,\frac{\partial \mu(X)}{\partial X} - \frac{\bar{F}}{\bar{V}}\right)\frac{\partial X}{\partial X_o} \qquad 3.27(a)$$

subject to $\left.\frac{\partial X}{\partial X_o}\right|_{t=0} = 1$

At the trivial state X = 0, and the equation becomes

$$\left(\frac{\partial \dot{X}}{\partial X_o}\right) = \left(\mu(S_F) - \frac{\bar{F}}{V_o + \bar{F}t}\right)\frac{\partial X}{\partial X_o} \qquad 3.27(b)$$

Integrating this we have $\left.\frac{\partial X}{\partial X_o}\right|_{t=t_f} = \frac{V_o}{V_f}\, e^{\mu(S)t_f}$

Hence the bifurcation point in terms of the dimensionless residence time is again $D^*_{cr} = (r-1)/\ln(r)$. Again two different bifurcation diagrams are possible. This depends upon the S_F value. These are depicted in Fig. 3.4 and 3.5.

The operation of the repeated fed-batch mode, with the instantaneous feeding and the constant flow-rate $\bar{F}$ are known to be suboptimal.

We now discuss the optimal performance of the repeated fed-batch reactor.

Case - I: In this case we consider the entire cycle time and the draw down ratio V_o/V_f to be externally fixed. This is solved by integrating equations 3.10a,b, 3.17a,b. The optimal profile is obtained when equations 3.20a are satisfied. This is ensured by iterating on w_i using 3.19.

The optimal flow-rate profiles for different values of ρ, are depicted in Fig. 3.6. For high values of ρ the optimal profile of

flow-rate is very close to the average flow-rate $\bar{F}$. This is only to be expected as now the weightage on the cost factor is high and the system tends to optimise the performance by minimising the cost rather than by maximising the productivity. As we decrease, ρ, it is seen that a larger variation in the flow-rate is permissible i.e. the deviation from the average flow-rate profile is high. This leads to a very significant improvement in the system performance i.e. biomass production. Here the system tends to optimise by improving the biomass production rather than by minimising the cost. A typical variation of the biomass concentration over a cycle is shown in Fig. 3.7. Since the imposed flow rate is bounded this variation is continuous. In particular the biomass at the end of the cycle and at the beginning are equal as opposed to the case of the intantaneous feed. This plot is for $\rho = 1.0$.

In Table 3.1 we compare the performances of the optimal profile with that of the fed-batch reactor filled at an average flow-rate $\bar{F}$, and the rapid fill fed-batch where the substrate is added instantaneously at the beginning of the cycle. The performance of the rapid fill case is the best and that with the average flow-rate $\bar{F}$ is very close to the optimal performance. This is the situation since the feed concentration here is lower than S^*.Since in this case the final volume and time are fixed the performance of reactors with $\bar{F}$, and instantaneous feed do not change, as they are independent of ρ.

The singular optimal control problem of repeated fed-batch mode of operation was investigated by Weigand[15]. The optimal

profile consisted of an instantaneous pulse feed, followed by a singular arc and then by a batch period. However, this is the optimal profile when $S_F > S^*$. The optimal profile for $S_F < S^*$ corresponds to the instantaneous filling of the reactor.

To study the effect of the parameter S_F on the optimal profile of our problem we simulated the optimisation for S_F = 14.75 > S^* (7.9). The optimal profile (Fig. 3.8) is of qualitatively different form. It consists of a portion where the flow-rate is almost a constant and greater than $\bar{F}$, followed by a period of batch operation. This is similar to the results of Weigand[15]. The flow-rate does not start of at an infinitely high value since we have a non-singular problem and also because we want to minimise the deviation from $\bar{F}$. The corresponding variation of biomass concentration is shown in Fig. 3.9.

This is in contrast to the optimal profile for $S_F < S^*$. Here the optimal profile is decreasing, and in the singular limit tends to the operation of rapid fill, repeated fed-batch reactor. In this mode the concentrations of substrate over a cycle is always less than S^*. Consequently the reaction behaves like it is governed by Monod kinetics (with monotonic dependency on S). The optimal operation hence is the instantaneous fill for this case.

The non-singular problem discussed here hence provides insight into the sequence of control actions of the classical singular problem as the parameter ρ tends to zero. Thus the profiles generated using our technique especially for low, ρ can be used to obtain insight into the different sequences of flow-rate profiles for the classical singular problem. This will

reduce the numerical scheme to determining only the "switching times between the different control actions."

In Fig. 3.10 we depict the performance of the case where the cycle time is fixed but the final volume is not. Here we optimise the performance with respect to the draw down ratio as well.

The optimal profiles exhibit a similar trend i.e. decreasing trend as in Fig. 3.6. The optimal profile for the singular problem i.e. in the limit $\rho = 0$ is hence similar to that discussed in Weigand for this case also.

In Table 3.2 we compare the optimal performance with that of the reactors with a constant flow rate $\bar{F}$ and instantaneous feed rate for the optimal V_F obtained. The constant flow rate $\bar{F}$ used to compute the optimal profile is 0.3. However, the results reported for the case of constant $\bar{F}$ operation in the Table is such that $\bar{F}$ is the flow-rate which fills the reactor from V_o to the V_F calculated by the optimal profile over the cycle time.Here again the improvement in the performance is best for the rapid fill case and when we minimise the deviation from an average flow-rate the performance is not very good.In the limit of ρ tending to zero the optimal performance catches up with the instantaenous fill.

Also for the same ρ the optimal performance is better when the final volume is not fixed in comparison to the case when it is fixed. This is only to be expected since we have now optimised the performance with respect to the draw-down ratio.

3.7 Conclusions

In this work we have analysed the bifurcation feature of the repeated fed-batch reactor operated in sub-optimal modes. The reactor shows the same qualitative behaviour as that of a CSTR.

The critical dilution rate beyond which wash out occurs for the CSTR i.e. at $D^* = 1$. However, for the case of the rapid fill mode of operation, and the case where the flow rate is a constant the washout state is unstable for lower values of D^*_{cr}. The critical dilution rate is lowered. This value is obtained by using Floquet theory on the trivial state as $(r-1)/\ln(r)$.

We have also obtained the optimal reactor performance for the case of a fixed draw-down ratio and the case of an optimal draw-down ratio. The performance for the latter case is always better than that of the former. The optimal profile obtained using the method proposed here for low ρ, can be used to generate an insight into the sequence of operations for the classical singular problem. This insight can then be used to numerically calculate the optimal profile for the singular problem.

Table 2.1

Comparison of Performance ($X_f V_f$) for Different Cases Batch, Semi-Batch (Constant F) and Optimal Fed-batch

Case	X_o= 0.1, S_o = 0.142857*1.e-3, ρ = 4.0, S_f= 500, $\bar{F}$ = 0.3						
	t_o	t_f	V_o	V_f	$X_f V_f$ fed batch	$X_f V_f$ Semi-batch with const F	$X_f V_f$ batch
Fixed final time fixed final volume	0	10.0	7.0	10.0	1.2430	1.2259	0.9416
Fixed final time free final volume	0	10.0	7.0	9.8417	1.2636	1.2437	0.9508
Free final time fixed final volume	0	11.3375	7.0	10.0	1.3518	1.3213	0.9796
Free final time free final volume	0	32.2009	7.0	15.0809	2.5171	2.1317	1.2393

Table 2.2

Effect of ρ on the Biomass Production ($X_f V_f$) in Fed Batch Mode Comparison with Semi-Batch (Constant F) and Batch

Case	X_o= 0.1, S_o = 0.142857 * 1.e-3, S_f= 500, $\bar{F}$ = 0.3							
	ρ	t_o	t_f	V_o	V_f	$X_f V_f$ fed batch	$X_f V_f$ Semi-batch (const F)	$X_f V_f$ batch
Fixed final time fixed final volume	0.8	0	10.0	7.0	10.0	1.4081	1.2259	0.9416
Fixed final time free final volume	2.0	0	10.0	7.0	9.5798	1.3393	1.2769	0.9686
Free final time fixed final volume	3.0	0	12.2464	7.0	10.0	1.4554	1.3904	1.0064
Free final time free final volume	3.8	0	28.2330	7.0	13.6668	2.5578	2.0465	1.2078

Table 2.3

Effect of Initial Conditions on the Flow Rate Profile and Biomass Production for Fixed Final Time Fixed Final Volume

Case	$X_o = 0.1$, $t_f = 10.0$, $V_o = 7.0$, $V_f = 10.0$, $S^* = 7.9310$			
	ρ	S_o	S_f	$X_f V_f$ fed batch
1. $S^* < S_F < S_o$	0.05	15.0	10.0	2.3140
2. $S^* < S_o < S_F$	0.05	10.0	15.0	2.4454
3. $S_o < S^* < S_F$	0.8	0.142857 *1.e-3	25.0	2.1429
4. $S_o < S^* < S_F$	4.0	0.142857 *1.e-3	500	1.2430
5. $S_F < S^* < S_o$	0.8	25.0	0.142857 *1.e-3	2.0394
6. $S_o < S_F < S^*$	0.3	0.142857 *1.e-3	5.0	1.2113
7. $S_F < S_o < S^*$	0.3	5.0	0.142857 *1.e-3	2.2492

Table 3.1

Comparison of Biomass Production of the Case Fixed Final Volume, Fixed Final Time of Optimal F, Repeated Fed-Batch with Constant F and Rapid Fill.

Fixed time fixed volume

$X_o = 1.0$, $S_f = 2.0$, $Y = 0.8$, $\alpha = 1.0$, $\beta = 25.0$, $\gamma = 62.9$,

$V_o = 7.0$, $V_f = 10.0$, $t_f = 10.0$, $\bar{F} = 0.3$, $\mu_{max} = 5.2$

ρ	$X_f(V_f - V_o)$ (optimal)	$X_f(V_f - V_o)$ (const. F)	$X_f(V_f - V_o)$ (rapid fill)
10.0	3.5856	3.5816	4.0930
4.0	3.5916	3.5816	4.0930
1.0	3.6210	3.5816	4.0930

Table 3.2

Comparison of Biomass Production of the Case Free Final Volume, Fixed Final Time of Optimal F, Repeated Fed-Batch with Constant F and Rapid Fill.

Fixed time free volume

$X_o = 1.0$, $S_f = 2.0$, $Y = 0.8$, $\alpha = 1.0$, $\beta = 25.0$, $\gamma = 62.9$,

$V_o = 7.0$, $t_f = 10.0$, $\bar{F} = 0.3$, $\mu_{max} = 5.2$

ρ	$X_f(V_f - V_o)$ (optimal)	V_f (optimal)	$X_f(V_f - V_o)$ (const. F)	$X_f(V_f - V_o)$ (rapid fill)
10.0	3.9027	10.4414	3.8985	4.5294
4.0	4.2203	10.9859	4.2098	4.9877
1.0	4.6027	12.6362	4.5736	5.7232

References

1. Biegler, L.T. "Solution of Dynamic Optimisation, Problems by Successive Quadratic Programming and Orthogonal Collocation", Computer & Chemical Engineering, Vol. 8, No. 3/4 pp 243-248 (1984).
2. Bonte, P. Modak, J.M. Tayeb, Y.J. Lim, H.C., "Computational Algorithms for Optimal Fed Rates for a Class of Fed Batch Fermentation : Numerical Results for Penicillin and Cell Mass production", Biotechnology & Bioengineering, Vol. 28, pp 1408-1420 (1996).
3. Bryson, A.E. and Ho, Y., "Applied Optimal Control",Blaisdell,Waltham,MA,1969.
4. Cazzador, L., On the Optimal Control of Fed-Batch Reactors with Substrate-inhibited Kinetics", Biotechnol Bioeng., Vol. 31, pp 670-674 (1988).
5. Cuthrell, J.E., Biegler, L.T., "Simultaneous Optimisation and Solution Method for Batch Reactor Control Profiles", Computer & Chemical Engineering, Vol. 13, No. 1, pp 49-63 (1989).
6. Ince, E.L., "Ordinary Differential Equations", Dover Publications, New York, 1956.
7. Lee Jeawan and Parulekar Satish H. "Enhanced Production of α-Amylase in Fed Batch Cultures of Bacillus Subtilis TN106", Biotechnology & Bioengineering, Vol. 42, pp 1142-1150 (1993).
8. Levin, K.L., "Maximising the Product Distribution in Batch Reactors : Reactions in Parallel", Chemical Engineering Science, Vol. 47, pp 1751-1760 (1992).

9. Leis, J.R., Kramer, M.A., "Sensitivity Analysis of System of Differential and Algebraic Equations", Computers & Chemical Engineering, Vol. 9, No. 1, pp 93-96 (1985).

10. Morrison, K.R., Sargent, R.W.H., "Optimisation of Multistage Processes Described by Differential-Algebraic Equations", Lecture Notes in Mathematics, Vol. 12, pp 86-102 (1984).

11. Modak, J.M., Lim, H.C., Jayeb, Y.K., "General Characteristics of Optimal Feed Rate Profiles for Various Fed Batch Fermentation Processes", Biotechnology & Bioengineering Vol. 28, pp 1396-1407 (1986).

12. San, K.Y., Stephanopolous, G., "The Effect of Growth Rate Delays in Substrate-Inhibited Kinetics on the Optimal Profile of Fed Batch Fermentor", Biotechnology & Bioengineering, Vol. 26, pp. 1261-1264 (1984).

13. Shukla, P.K. and Pushpavanam, S., "Optimisation of Biochemical Reactors : An Analysis of Different Approximations of Fed Batch Operation", submitted for publication for Chemical Engineering Science (June 1996).

14. Vassiliadis, V.S., Sargent, R.W.H., and Pantelides, C.C., "Solution of a Class of Multistage Dynamic Optimisation Problem 1 : Problems without Path Constraints", Ind. & Eng. Chem. Res., Vol. 33, pp 2111-2122 (1984).

15. Weigand, W.A., "Maximum Cell Productivity by Repeated Fed-Batch Culture Yield Case", Biotech. & Bioengg. Vol. 23, pp 249-266 (1981).

16. Westage, J. Paul, Curtis, R. Wayne, Emergy. H. Alden, Hasegawa. M. and paul and Heinstein Peter F., "Approximation of Continuous Growth of Cephalotaxus Harringtonia Plant Cell Cultures Using Fed Batch Concentrations", Biotechnology & Bioengineering, Vol. 38, pp 241-246 (1991).

APPENDIX I

The equation (2.7) is substituted back in equation 2.3(a), 2.3(b), 2.5, 2.6(a), 2.6(b). The senstivity is determined with respect to λ_{xo}, λ_{vo} , by differentiating the evoluation equations with respect to λ_{xo}, λ_{vo} for cases I & II. This yields

$$\frac{\partial \dot{X}}{\partial \lambda_{xo}} = \left[\mu(g(X,V)) + X \frac{\partial \mu(g(X,V))}{\partial X} - \frac{F}{V} \right] \frac{\partial X}{\partial \lambda_{xo}} + \left[X \frac{\partial \mu(g(X,V))}{\partial V} + \frac{FX}{V^2} \right] \frac{\partial V}{\partial \lambda_{xo}} - \frac{X}{V} \frac{\partial F}{\partial \lambda_{xo}} \qquad 2.1(a)$$

$$\frac{\partial \dot{X}}{\partial \lambda_{vo}} = \left[\mu(g(X,V)) + X \frac{\partial \mu(g(X,V))}{\partial X} - \frac{F}{V} \right] \frac{\partial X}{\partial \lambda_{vo}} + \left[X \frac{\partial \mu(g(X,V))}{\partial V} + \frac{FX}{V^2} \right] \frac{\partial V}{\partial \lambda_{vo}} - \frac{X}{V} \frac{\partial F}{\partial \lambda_{vo}} \qquad 2.1(b)$$

$$\frac{\partial \dot{V}}{\partial \lambda_{xo}} = \frac{\partial F}{\partial \lambda_{xo}} \qquad 2.1(c)$$

$$\frac{\partial \dot{V}}{\partial \lambda_{vo}} = \frac{\partial F}{\partial \lambda_{vo}} \qquad 2.1(d)$$

$$\frac{\partial \dot{\lambda}_x}{\partial \lambda_{xo}} = - \lambda_x \left[2 \frac{\partial \mu(g(X,V))}{\partial X} + X \frac{\partial^2 \mu(g(X,V))}{\partial X^2} \right] \frac{\partial X}{\partial \lambda_{xo}} - \lambda_x \left[\frac{\partial \mu(g(X,V))}{\partial V} + X \frac{\partial^2 \mu(g(X,V))}{\partial V \partial X} + \frac{F}{V^2} \right] \frac{\partial V}{\partial \lambda_{xo}} - \left[\mu(g(X,V)) + X \frac{\partial \mu(g(X,V))}{\partial X} - \frac{F}{V} \right] \frac{\partial \lambda_x}{\partial \lambda_{xo}} + \frac{\lambda_x}{V} \frac{\partial F}{\partial \lambda_{xo}} \qquad 2.1(e)$$

$$\frac{\partial \dot{\lambda}_x}{\partial \lambda_{vo}} = -\lambda_x \left[2\frac{\partial \mu(g(X,V))}{\partial V} + X\frac{\partial^2 \mu(g(X,V))}{\partial X^2}\right]\frac{\partial X}{\partial \lambda_{vo}}$$

$$-\lambda_x \left[\frac{\partial \mu(g(X,V))}{\partial V} + X\frac{\partial^2 \mu(g(X,V))}{\partial V \partial X} + \frac{F}{V^2}\right]\frac{\partial V}{\partial \lambda_{vo}}$$

$$-\left[\mu(g(X,V)) + X\frac{\partial \mu(g(X,V))}{\partial X} - \frac{F}{V}\right]\frac{\partial \lambda_x}{\partial \lambda_{vo}}$$

$$+\frac{\lambda_x}{V}\frac{\partial \lambda_x}{\partial \lambda_{vo}} \qquad 2.1(f)$$

$$\frac{\partial \dot{\lambda}_v}{\partial \lambda_{xo}} = -\lambda_x \left[\frac{\partial \mu(g(X,V))}{\partial V} + X\frac{\partial^2 \mu(g(X,V))}{\partial X \partial V} + \frac{F}{V^2}\right]\frac{\partial X}{\partial \lambda_{vo}}$$

$$-\lambda_x \left[X\frac{\partial^2 \mu(g(X,V))}{\partial V^2} - \frac{2FX}{V^3}\right]\frac{\partial V}{\partial \lambda_{xo}}$$

$$-\left[\frac{X\partial \mu(g(X,V))}{\partial V} + \frac{FX}{V^2}\right]\frac{\partial \lambda_x}{\partial \lambda_{xo}} - \frac{\lambda_x X}{V^2}\frac{\partial F}{\partial \lambda_{xo}} \qquad 2.1(g)$$

$$\frac{\partial \dot{\lambda}_v}{\partial \lambda_{vo}} = -\lambda_x \left[\frac{\partial \mu(g(X,V))}{\partial V} + X\frac{\partial^2 \mu(g(X,V))}{\partial X \partial V} + \frac{F}{V^2}\right]\frac{\partial X}{\partial \lambda_{vo}}$$

$$-\lambda_x \left[X\frac{\partial^2 \mu(g(X,V))}{\partial V^2} - \frac{2FX}{V^3}\right]\frac{\partial V}{\partial \lambda_{vo}}$$

$$-\left[X\frac{\partial \mu(g(X,V))}{\partial V} + \frac{FX}{V^2}\right]\frac{\partial \lambda_x}{\partial \lambda_{vo}} - \frac{\lambda_x X}{V^2}\frac{\partial F}{\partial \lambda_{vo}} \qquad 2.1(h)$$

The equation $\frac{\partial F}{\partial \lambda_{xo}}$ and $\frac{\partial F}{\partial \lambda_{vo}}$ are given by

$$\frac{\partial F}{\partial \lambda_{xo}} = \frac{1}{2\rho}\left[\left(\frac{\lambda_x}{V}\right)\frac{\partial X}{\partial \lambda_{xo}} - \left(\frac{\lambda_x X}{V^2}\right)\frac{\partial V}{\partial \lambda_{xo}} + \left(\frac{X}{V}\right)\frac{\partial \lambda_x}{\partial \lambda_{xo}} - \frac{\partial \lambda_v}{\partial \lambda_{xo}}\right] \qquad 2.1(i)$$

$$\frac{\partial F}{\partial \lambda_{vo}} = \frac{1}{2\rho}\left[\left(\frac{\lambda_x}{V}\right)\frac{\partial X}{\partial \lambda_{vo}} - \left(\frac{\lambda_x X}{V^2}\right)\frac{\partial V}{\partial \lambda_{xo}} + \left(\frac{X}{V}\right)\frac{\partial \lambda_x}{\partial \lambda_{vo}} - \frac{\partial \lambda_v}{\partial \lambda_{vo}}\right] \qquad 2.1(j)$$

APPENDIX II

The sensitivity equations required for case (3) and (4) besides the equation given in Appendix I are :

$$\frac{\partial H}{\partial \lambda_{xo}} = \left[X\mu(g(X,V)) - \frac{FX}{V}\right] \frac{\partial \lambda_x}{\partial \lambda_{xo}} + \lambda_x \left[\mu(g(X,V)) + X \frac{\partial \mu(g(X,V))}{\partial X} - \frac{F}{V}\right] \frac{\partial X}{\partial \lambda_{xo}}$$

$$+ \lambda_x \left[X \frac{\partial \mu(g(X,V))}{\partial V} + \frac{FX}{V^2}\right] \frac{\partial V}{\partial \lambda_{xo}} + F \frac{\partial \lambda_v}{\partial \lambda_{xo}}$$

$$+ \left[-\frac{\lambda_x X}{V} + \lambda_v + 2\rho\ (F - \bar{F})\right] \frac{\partial F}{\partial \lambda_{xo}} \qquad 2.1(k)$$

$$\frac{\partial H}{\partial \lambda_{vo}} = \left[X\mu(g(X,V)) - \frac{FX}{V}\right] \frac{\partial \lambda_x}{\partial \lambda_{vo}} + \lambda_x \left[\mu(g(X,V)) + X \frac{\partial \mu(g(X,V))}{\partial X} - \frac{F}{V}\right] \frac{\partial X}{\partial \lambda_{vo}}$$

$$+ \lambda_x \left[X \frac{\partial \mu(g(X,V))}{\partial V} + \frac{FX}{V^2}\right] \frac{\partial V}{\partial \lambda_{vo}} + F \frac{\partial \lambda_v}{\partial \lambda_{vo}}$$

$$+ \left[-\frac{\lambda_x X}{V} + \lambda_v + 2\rho\ (F - \bar{F})\right] \frac{\partial F}{\partial \lambda_{vo}} \qquad 2.1(l)$$

$$\frac{\partial H}{\partial t} = \left[X\mu(g(X,V)) - \frac{FX}{V}\right] \frac{\partial \lambda_x}{\partial t} + \lambda_x \left[\mu(g(X,V)) - \frac{F}{V} + X \frac{\partial \mu(g(X,V))}{\partial X}\right] \frac{\partial X}{\partial t} + F \frac{\partial \lambda_v}{\partial t} + \lambda_x \left[X \frac{\partial \mu(g(X,V))}{\partial V} + \frac{FX}{V^2}\right] \frac{\partial V}{\partial t}$$

$$+ \left[-\frac{\lambda_x X}{V} + \lambda_v + 2\rho\ (F - \bar{F})\right] \frac{\partial F}{\partial t} \qquad 2.1(m)$$

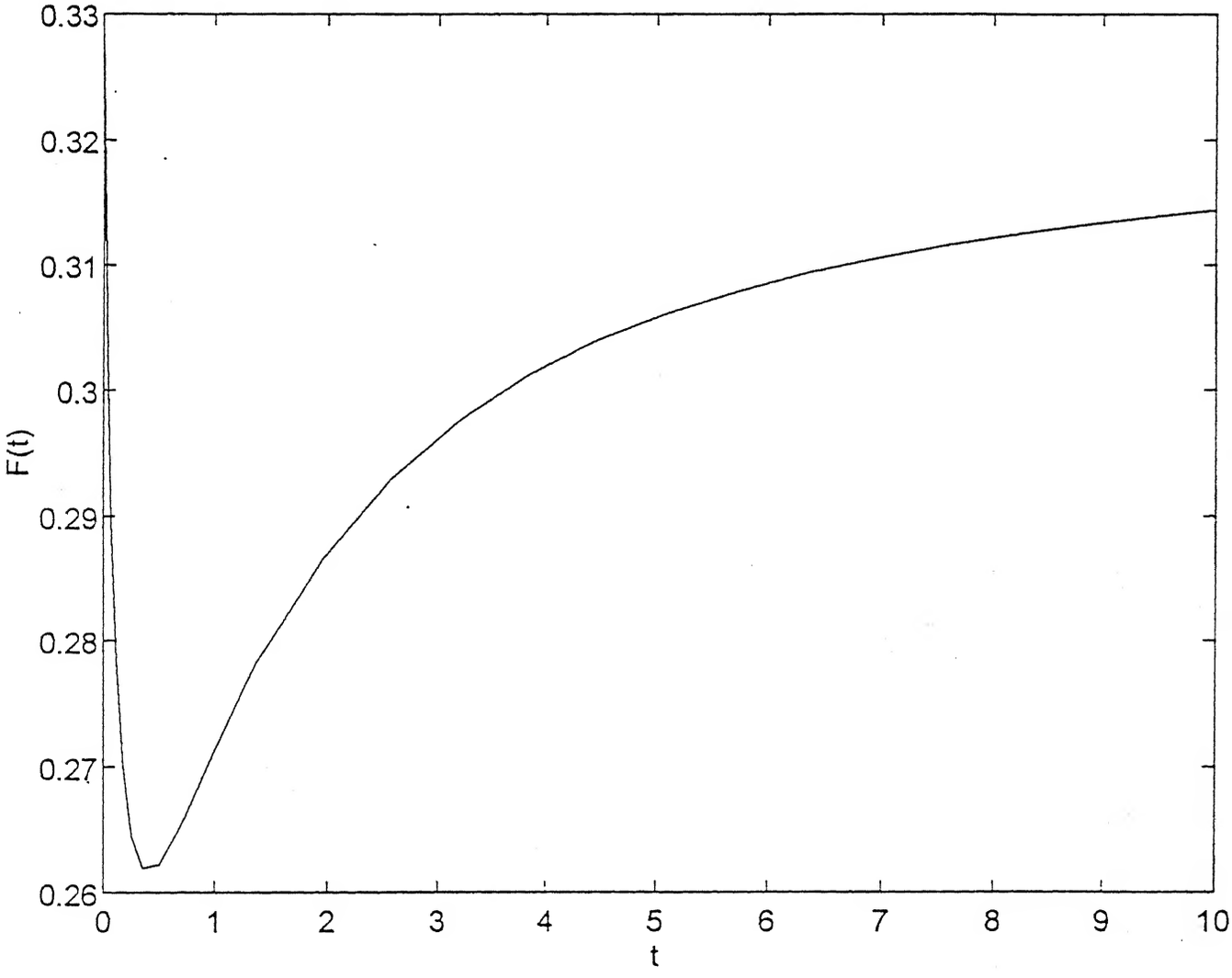

Fig. 2.1: Flow rate profile for case I for $\rho = 4.0$ for biomass production.

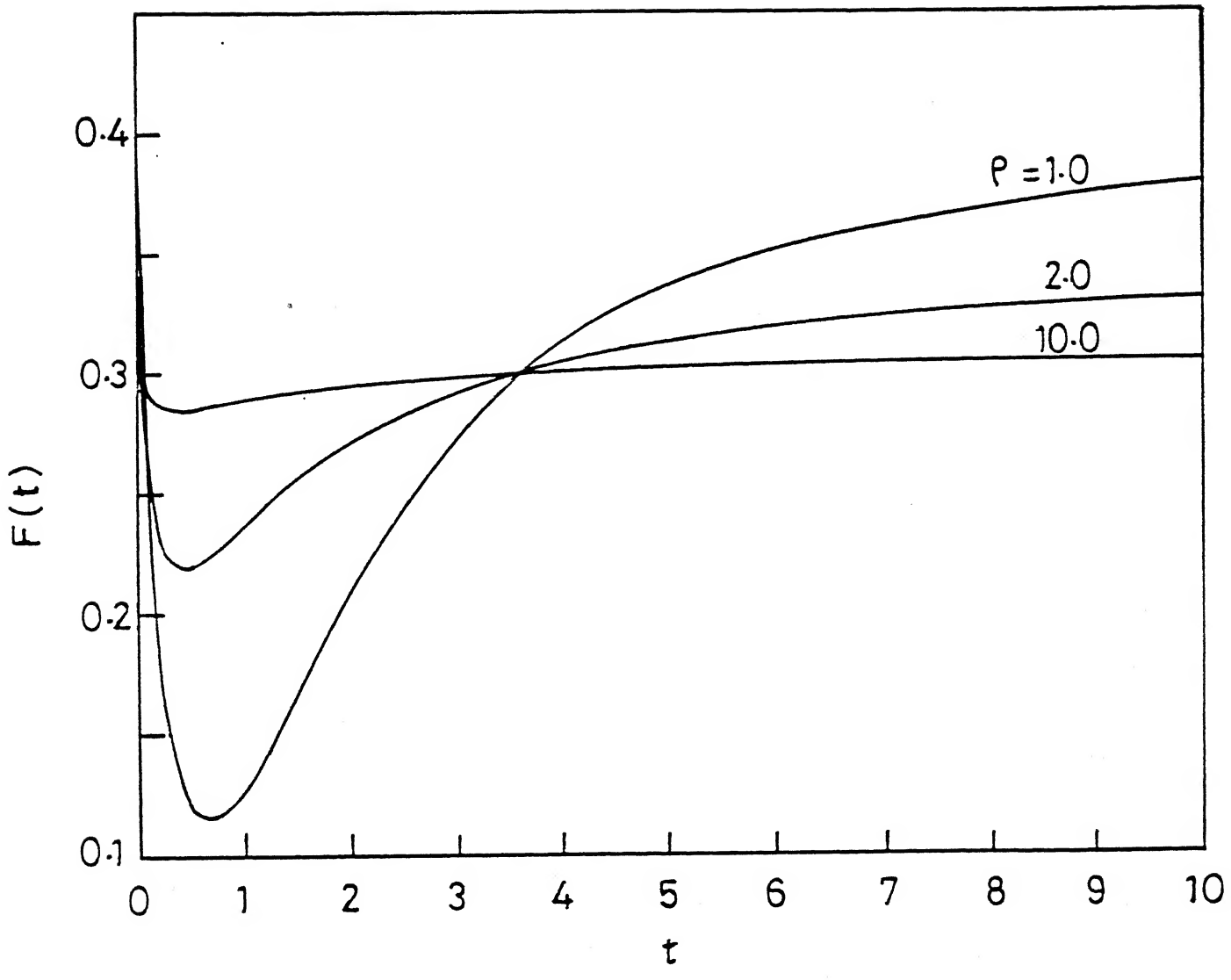

Fig. 2.2: Effect of ρ on the biomass production for case I.

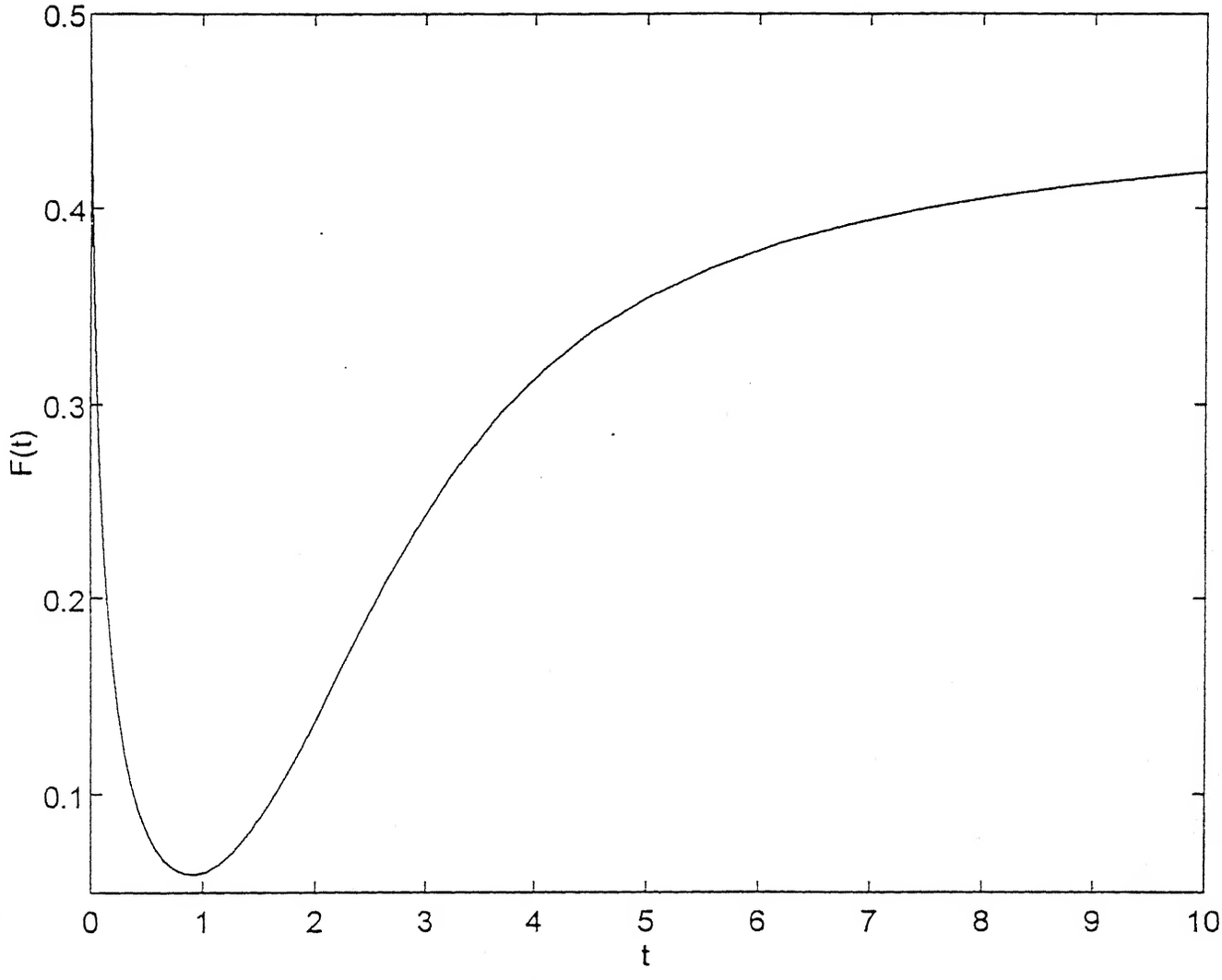

Fig. 2.3: Flow rate profile (see Table 2.2 for numeric data)

(a) Case I

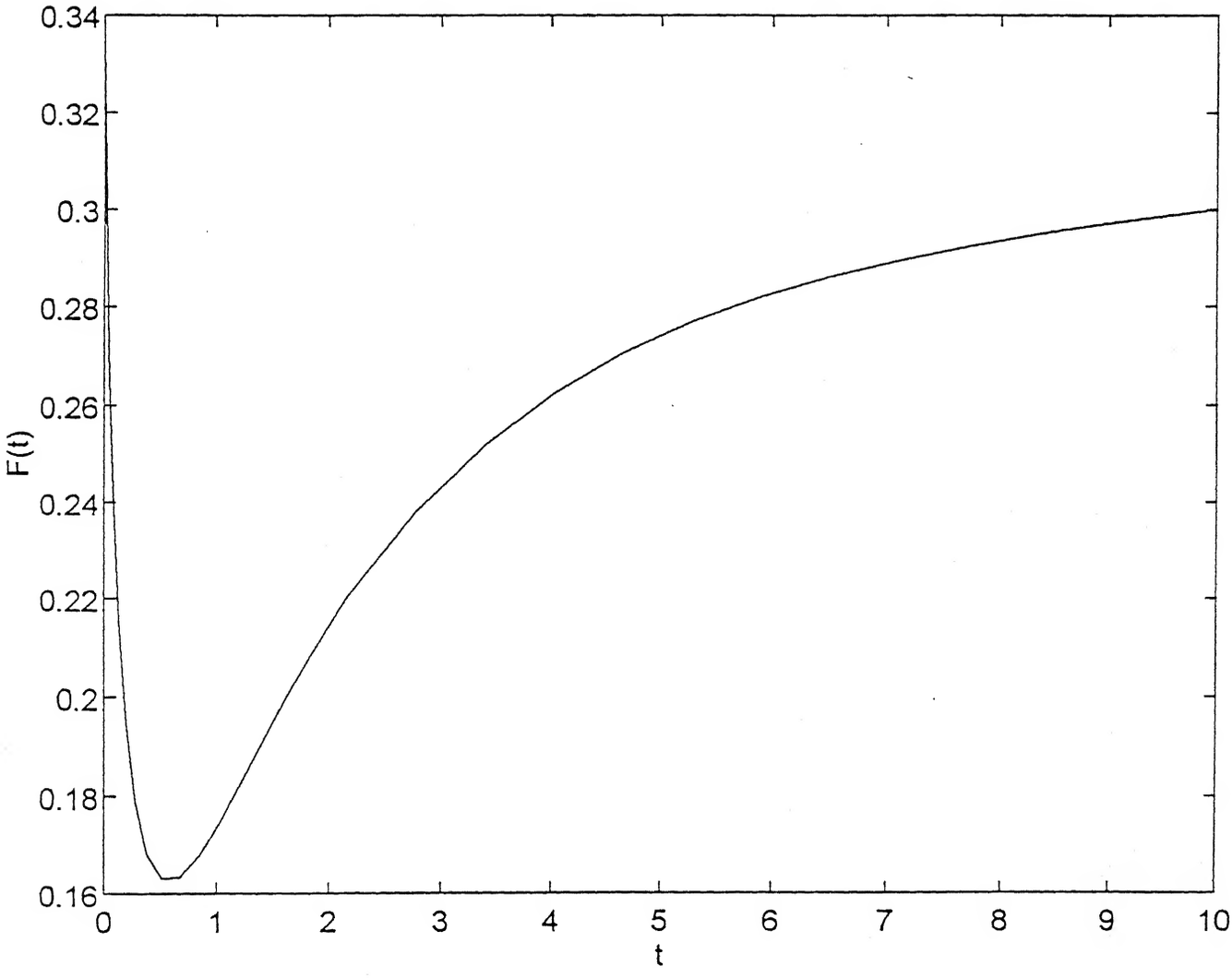

Fig. 2.3: Flow rate profile (see Table 2.2 for numeric data)

(b) Case II

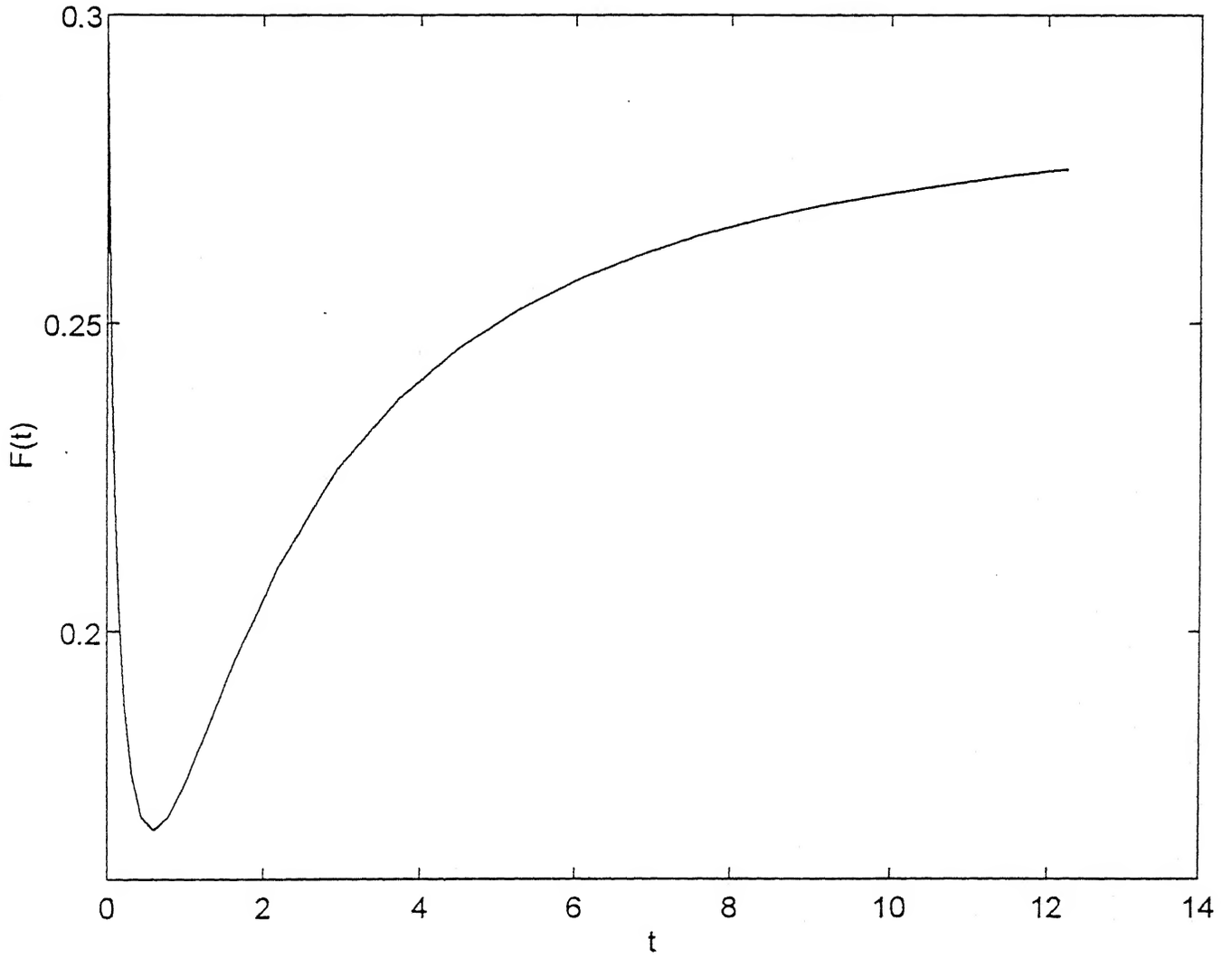

Fig. 2.3: Flow rate profile (see Table 2.2 for numeric data)

(c) Case III

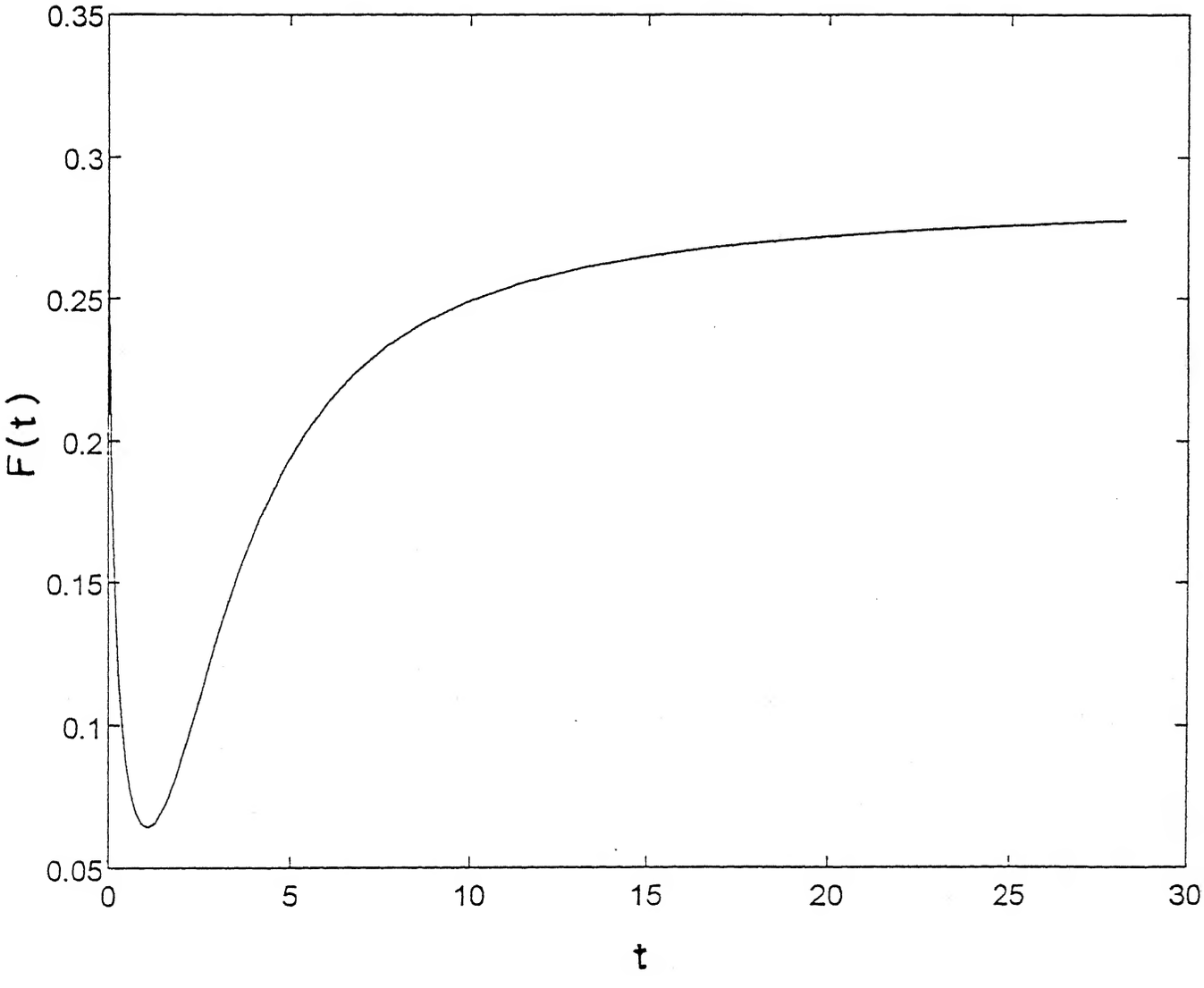

Fig. 2.3: Flow rate profile (see Table 2.2 for numeric data)

(d) Case IV

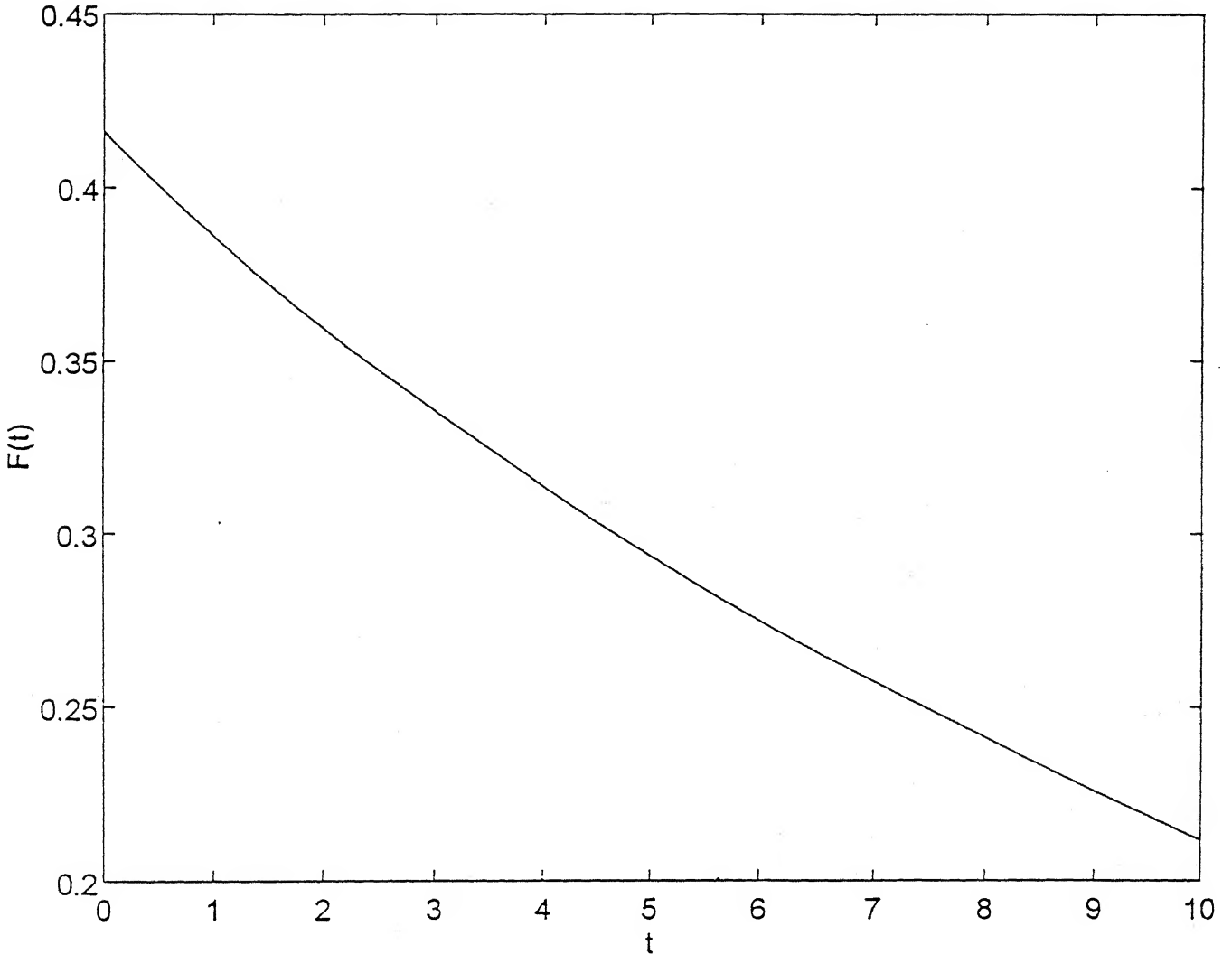

Fig. 2.4: Flow rate profile (see Table 2.3 for numeric data)

(a) $S^* < S_F < S_o$

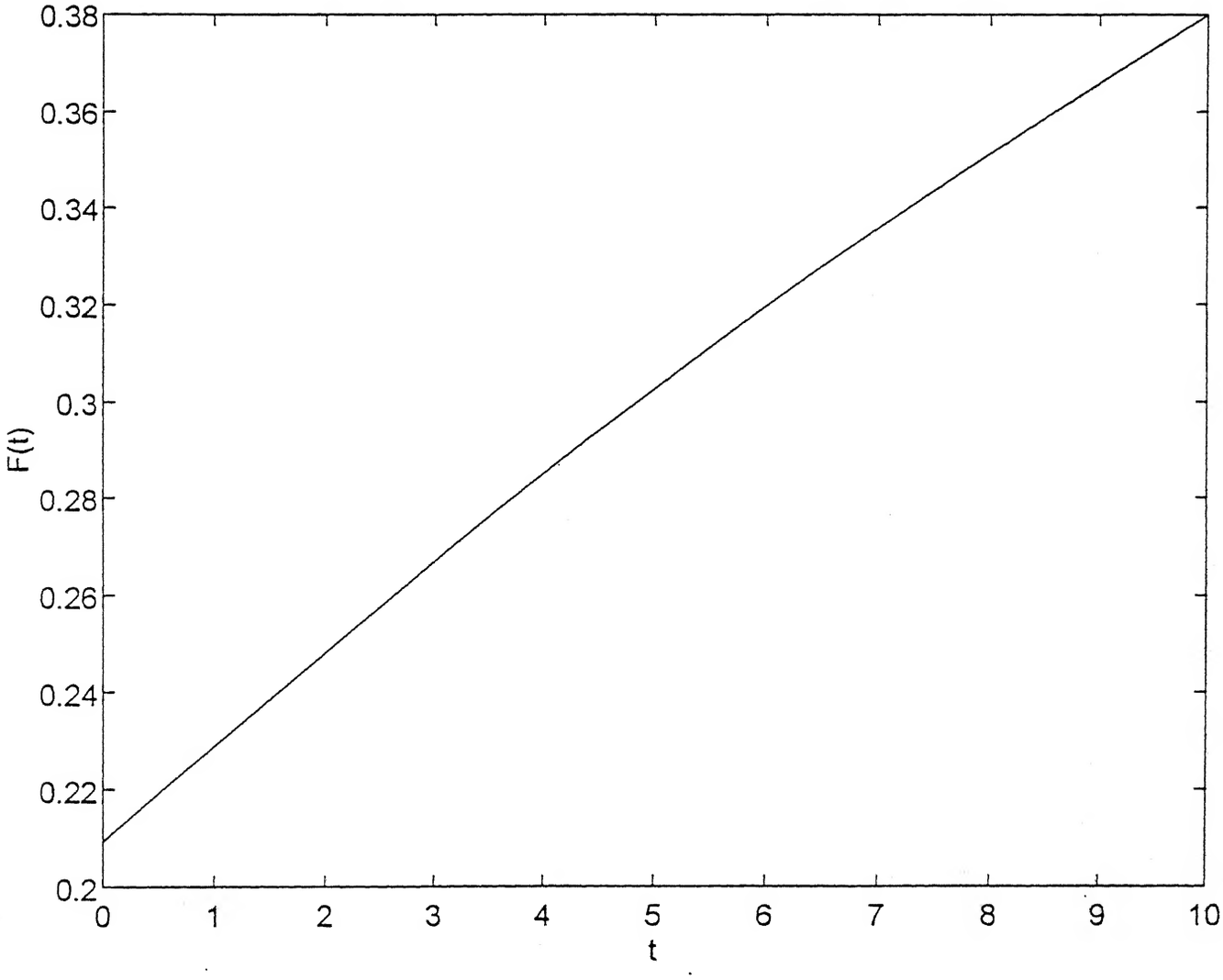

Fig. 2.4: Flow rate profile (see Table 2.3 for numeric data)

(b) $S^* < S_o < S_F$

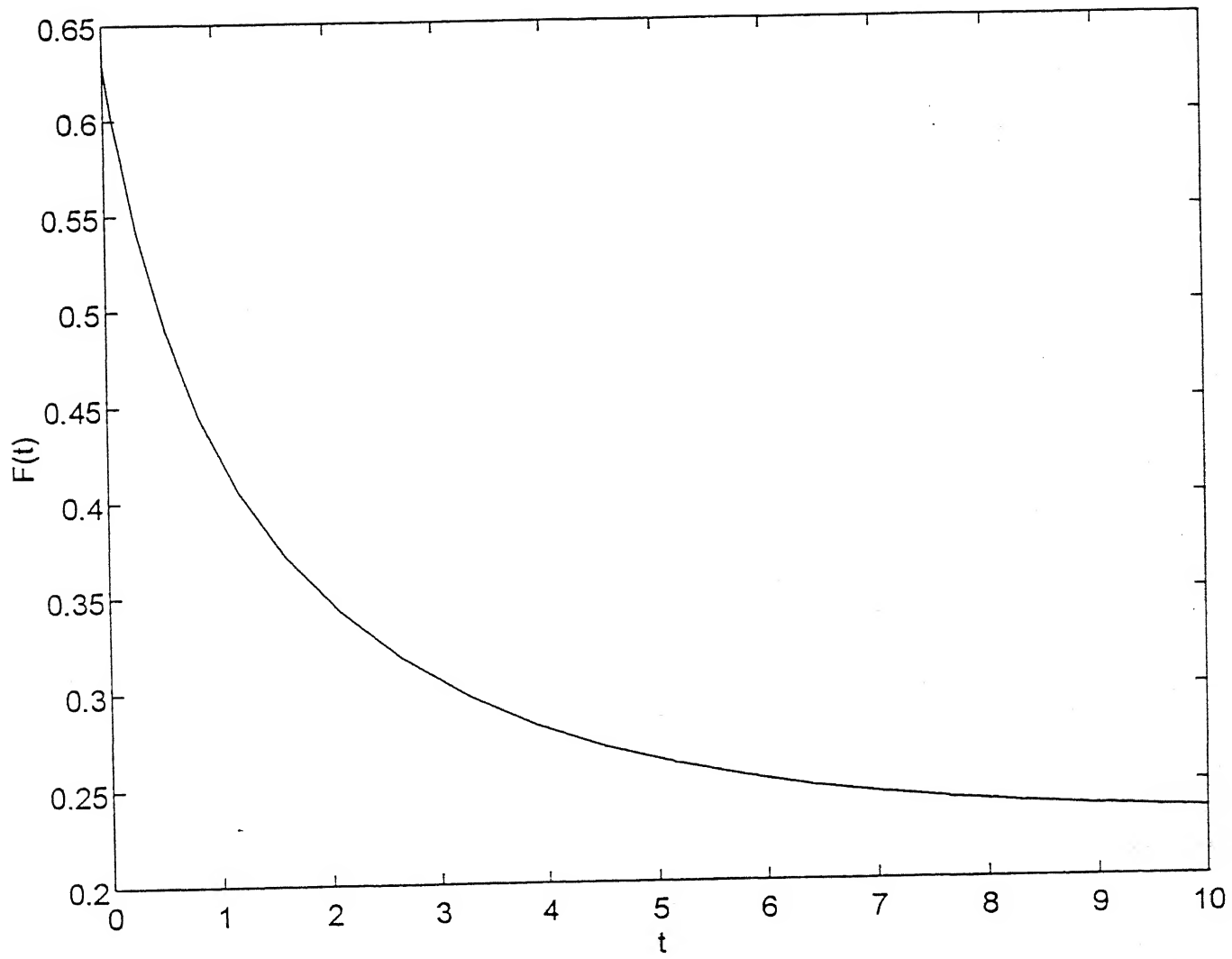

Fig. 2.4: Flow rate profile (see Table 2.3 for numeric data)

(c) $S_0 < S^* < S_F$

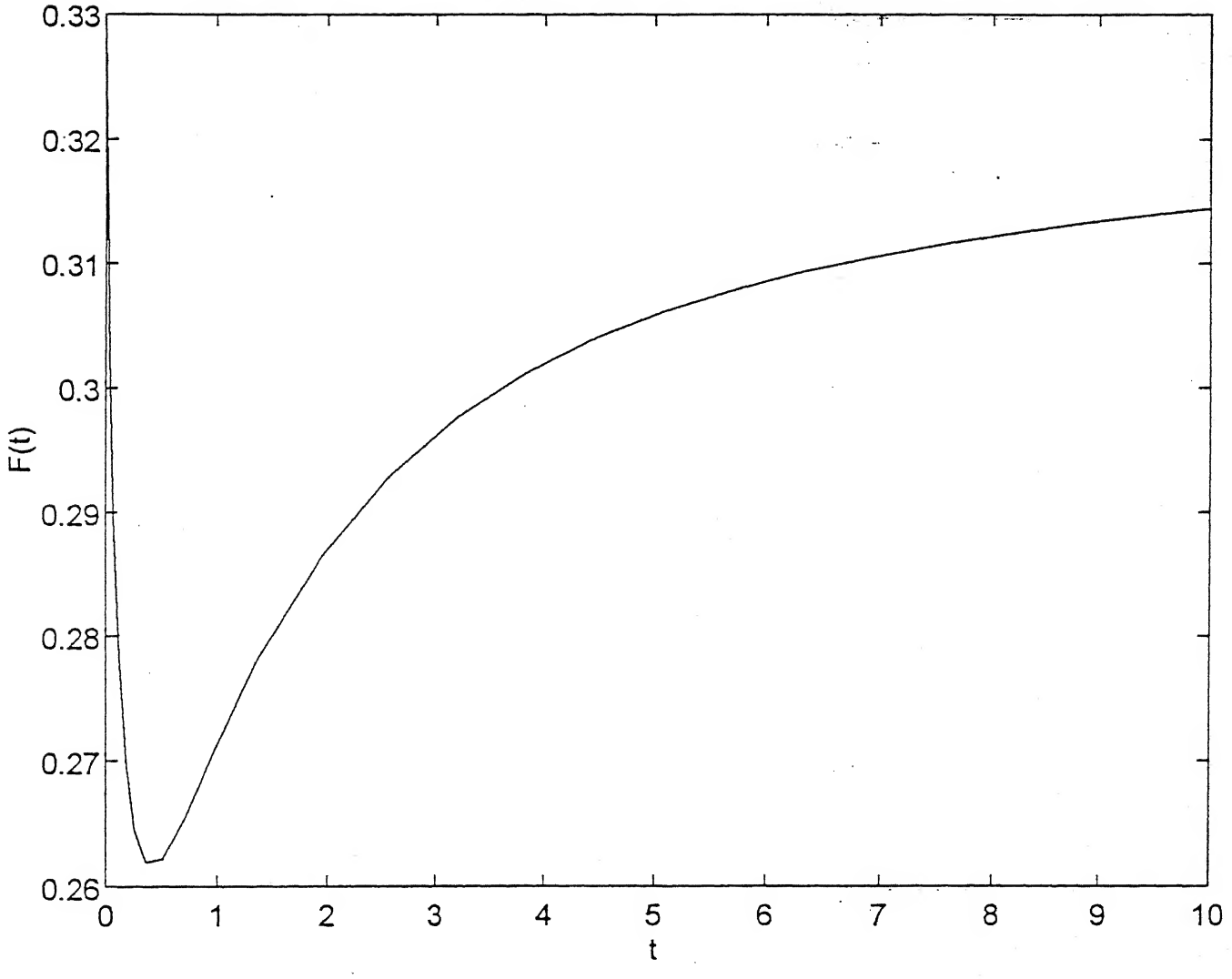

Fig. 2.4: Flow rate profile (see Table 2.3 for numeric data)

(d) $S_o < S^* < S_F$

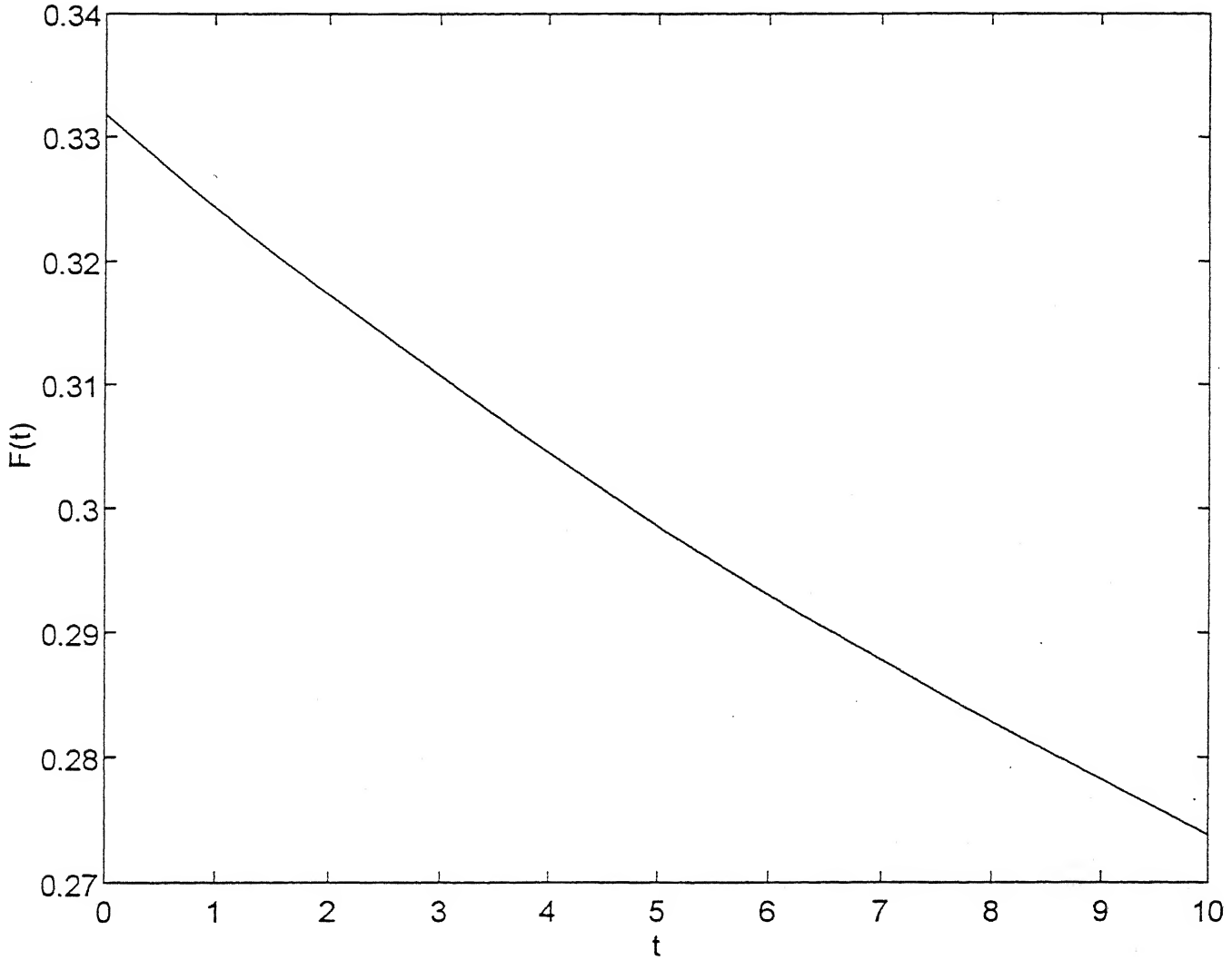

Fig. 2.4: Flow rate profile (see Table 2.3 for numeric data)

(a) $S_F < S^* < S_o$

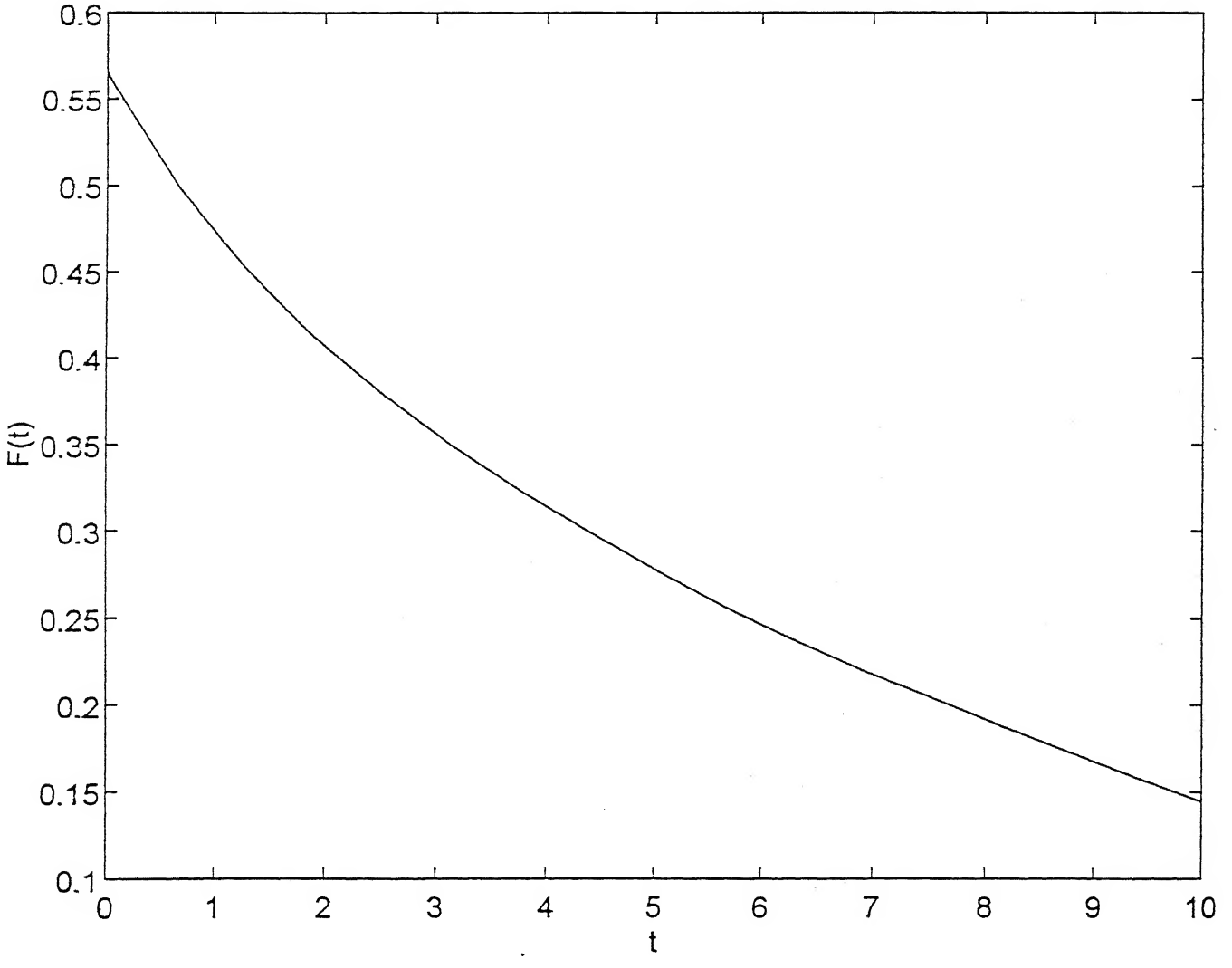

Fig. 2.4: Flow rate profile (see Table 2.3 for numeric data)

(f) $S_o < S_F < S^*$

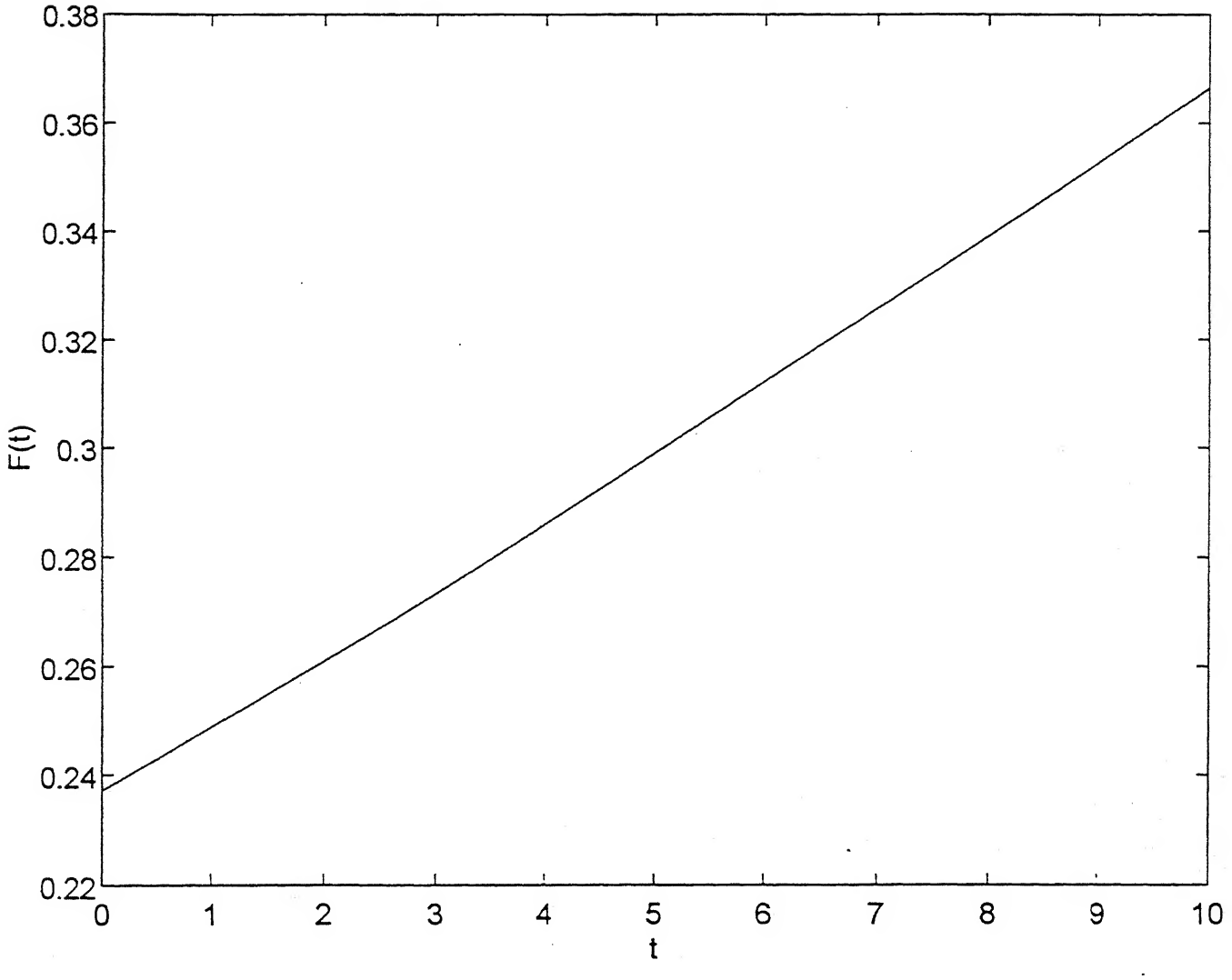

Fig. 2.4: Flow rate profile (see Table 2.3 for numeric data)

(g) $S_f < S_o < S^*$

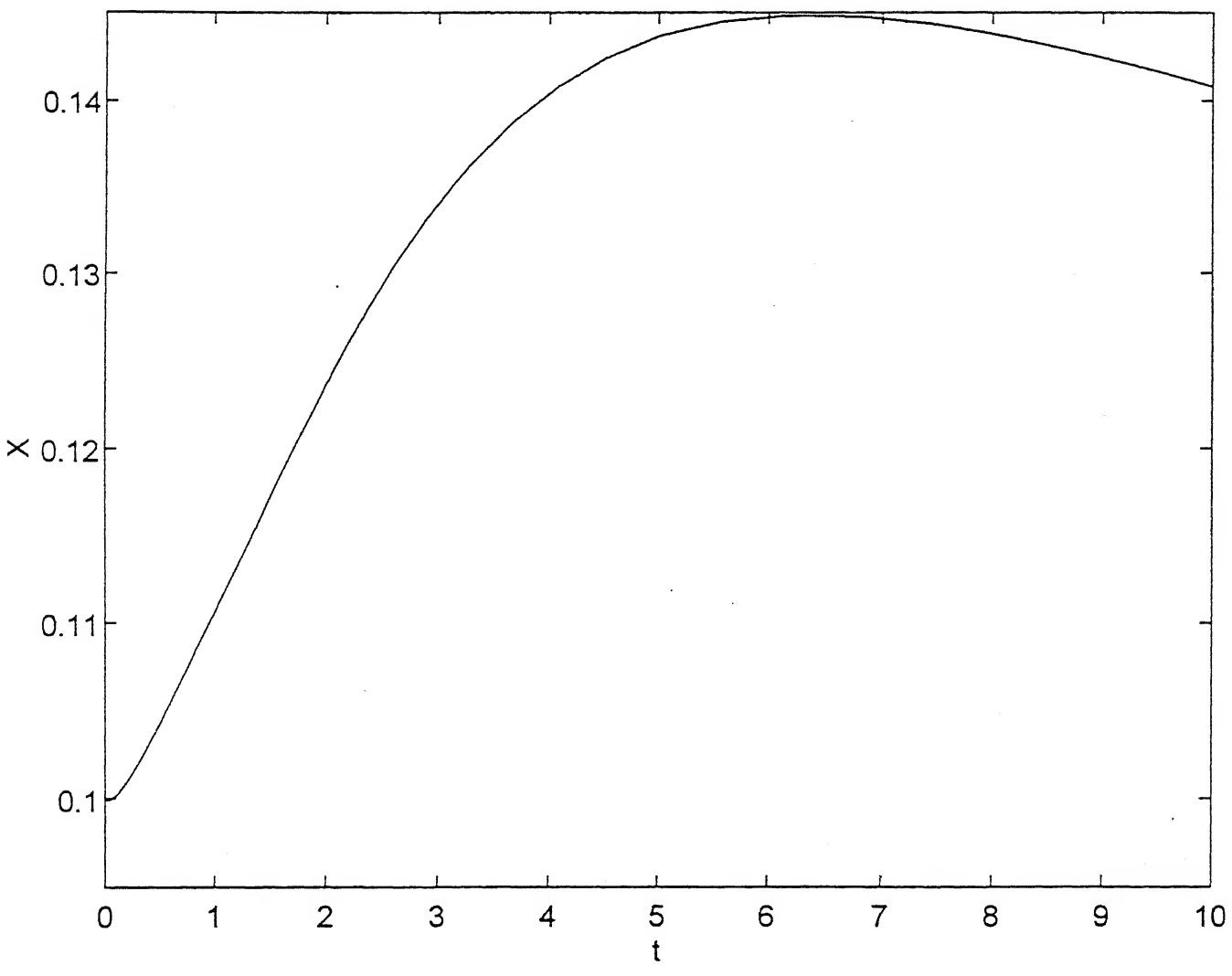

Fig. 2.5: Variation of Biomass concentration with time for the flow-rate profile in Fig. 2.3a.

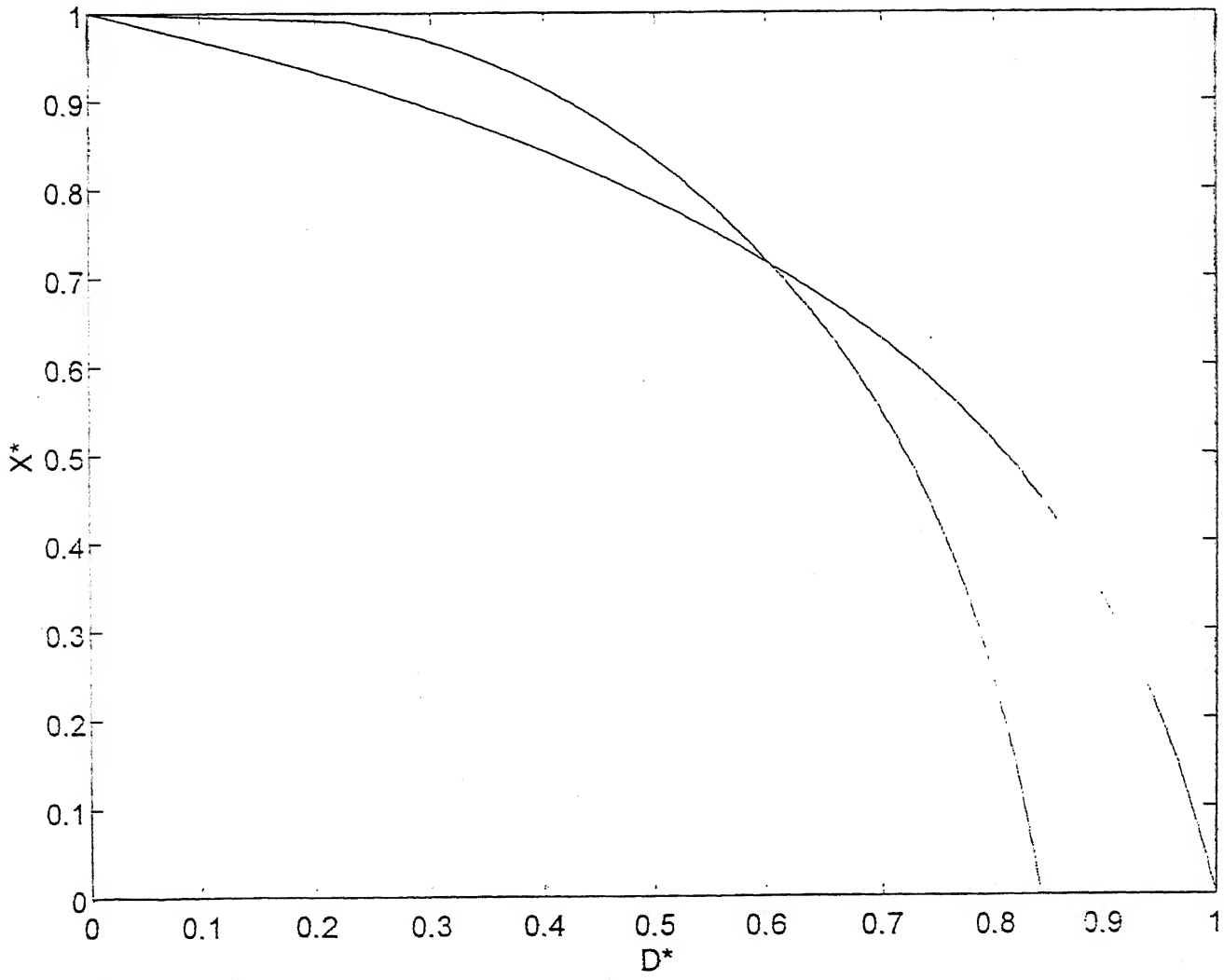

Fig. 3.1: Comparison of the bifurcation diagram of a CSTR and a rapid fill RFB when $S_F < S^*$, $S_F = 5.0$, $r = 0.7$.

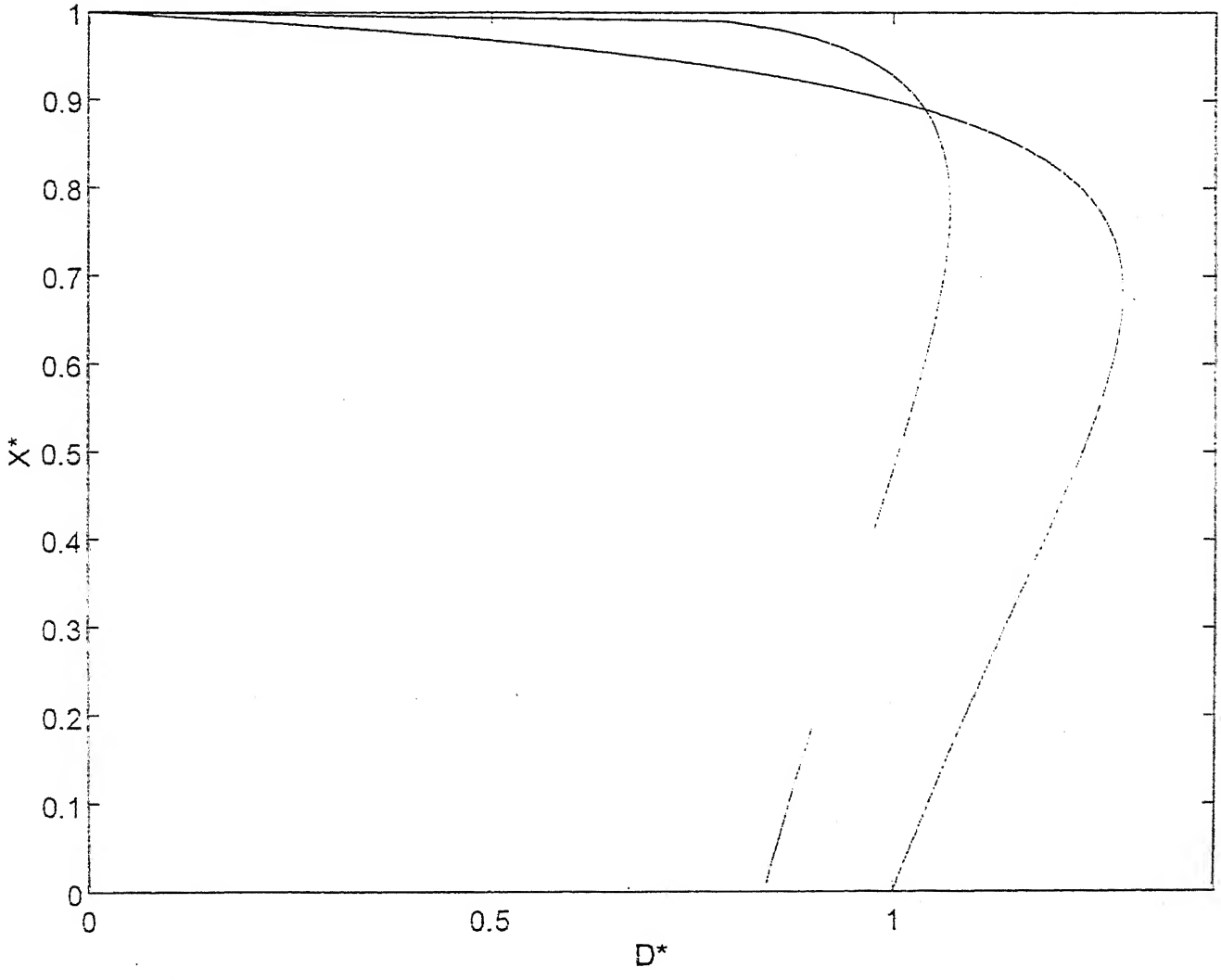

Fig. 3.2: Comparison of the bifurcation diagram of a CSTR and a rapid fill RFB when $S_F > S^*$, $S_F = 15.0$, $r = 0.7$.

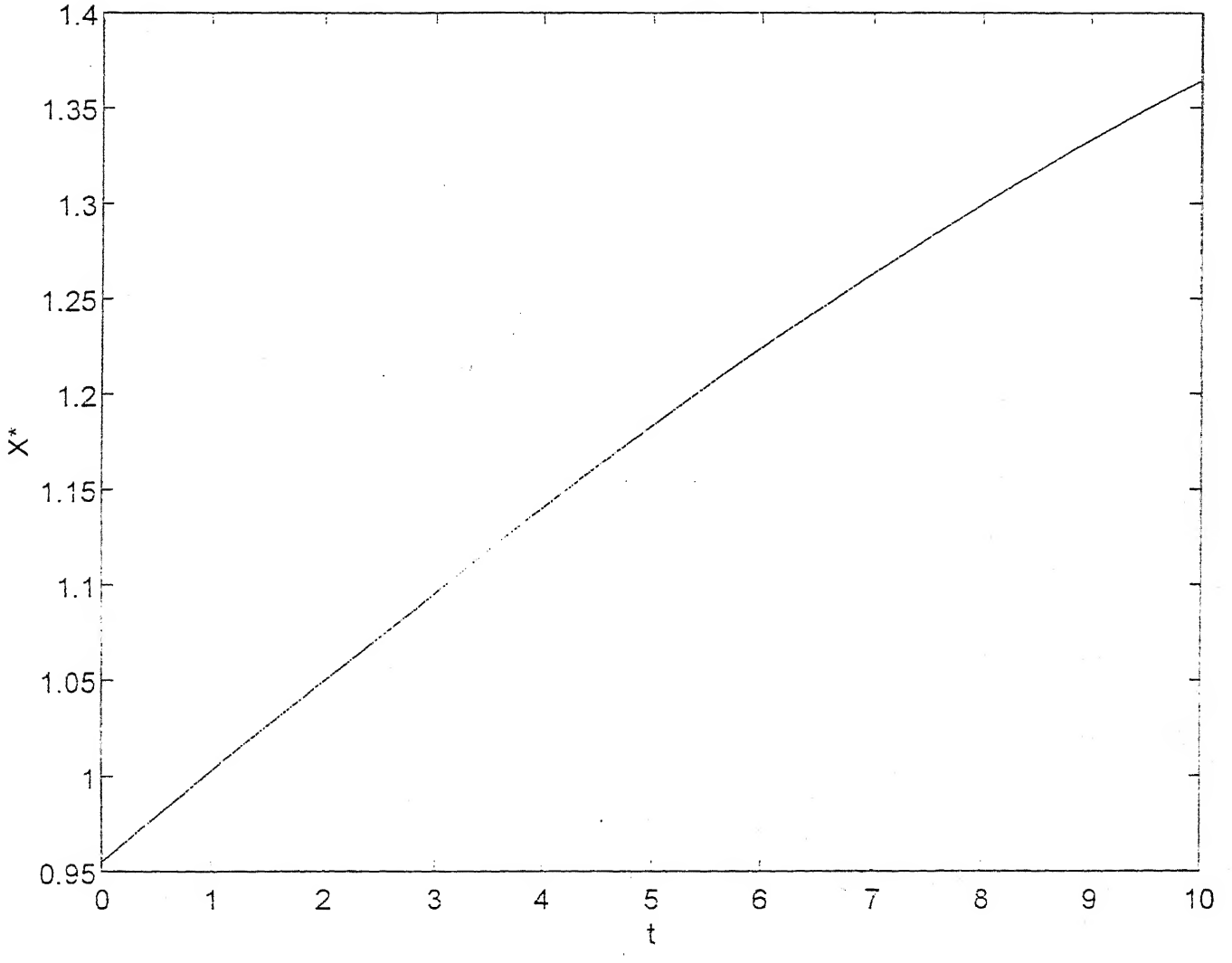

Fig. 3.3: Plot of X vs. time for a rapid fill RFB for r = 0.7.

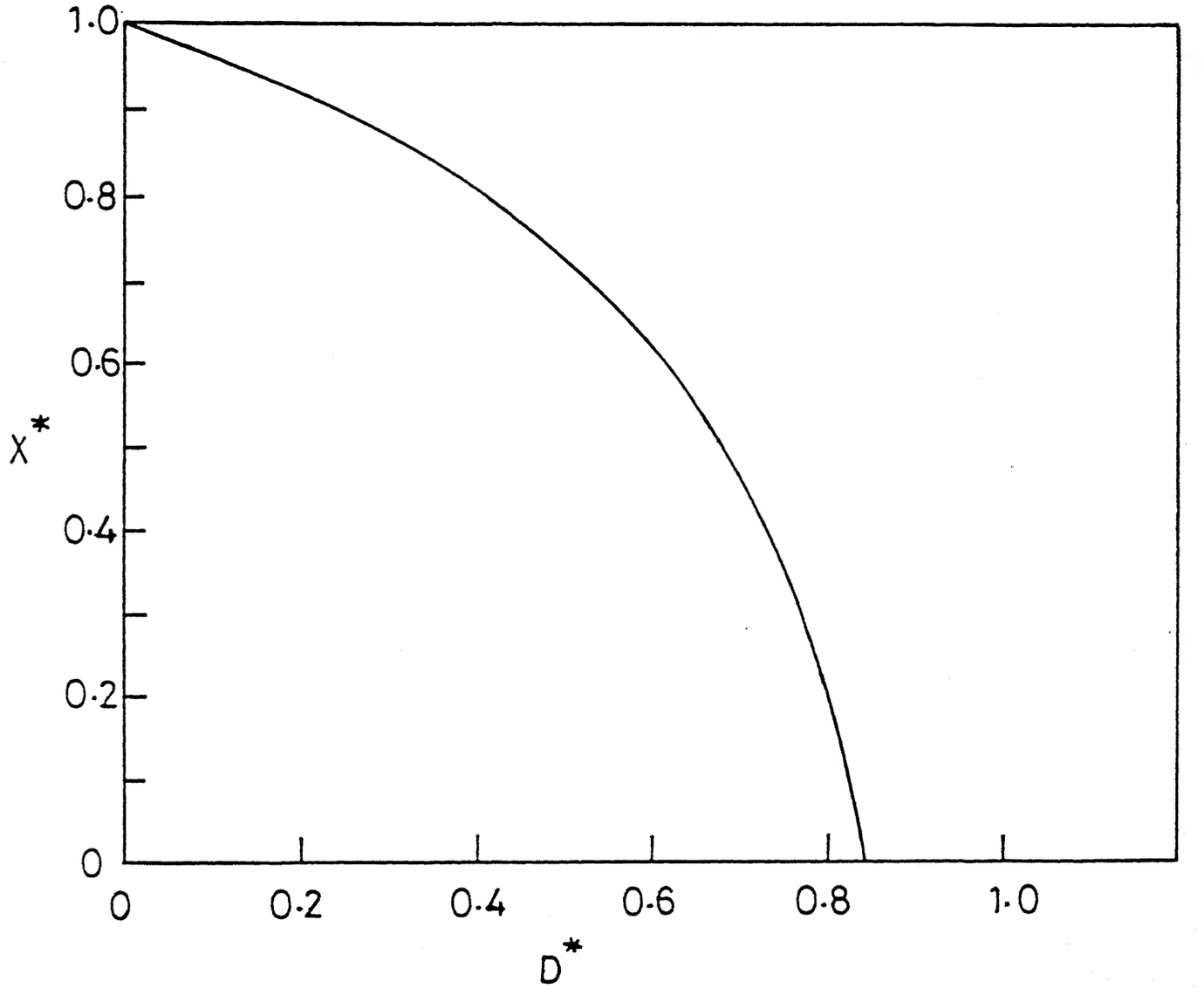

Fig. 3.4: Bifurcation diagram of a repeated fed-batch, constant $\bar{F}$ when $S_F < S^*$, $S_F = 5$, $r = 0.7$.

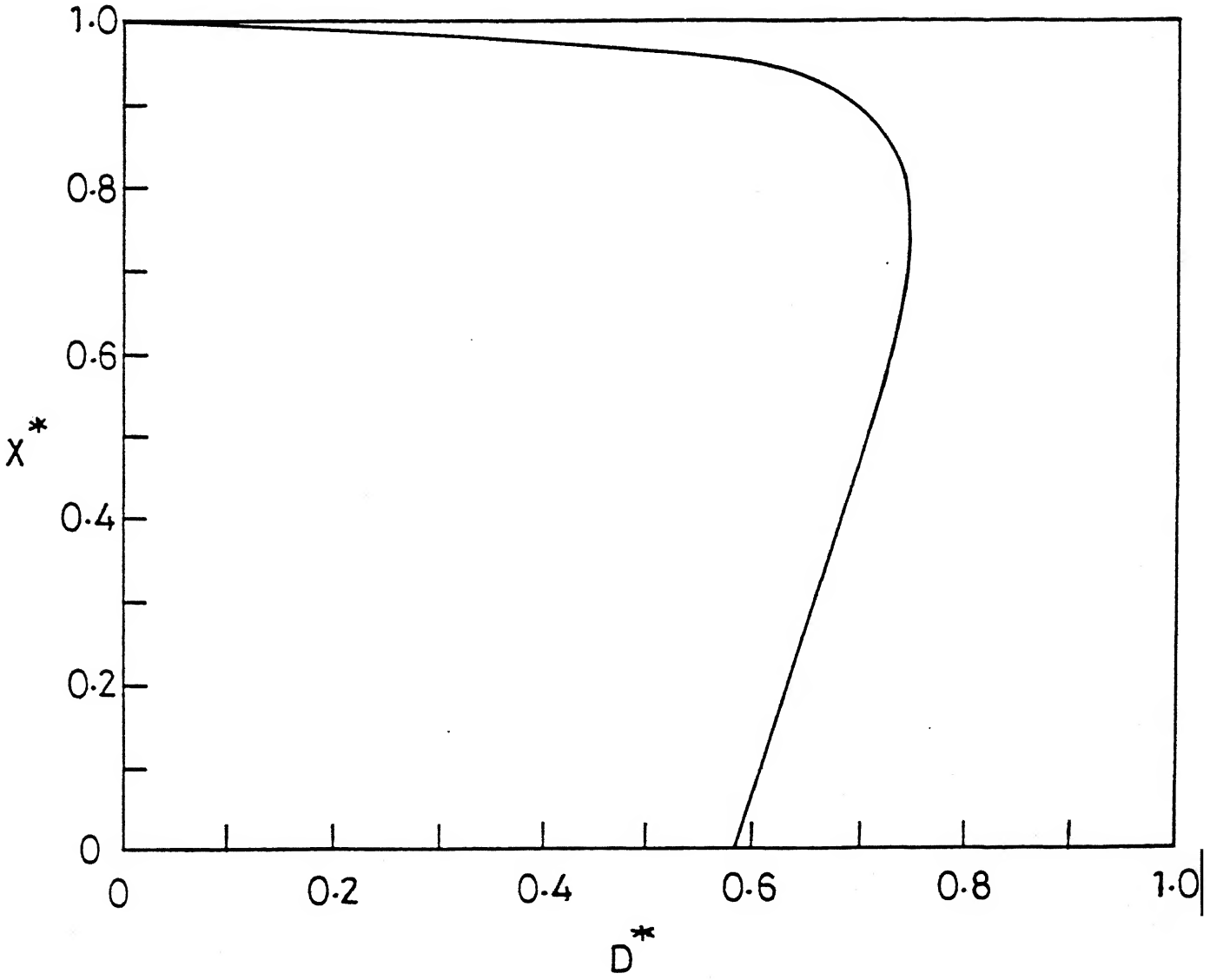

Fig. 3.5: Bifurcation diagram of a repeated fed-batch, constant $\bar{F}$ when $S_F > S^*$, $S_F = 25$, $r = 0.3$.

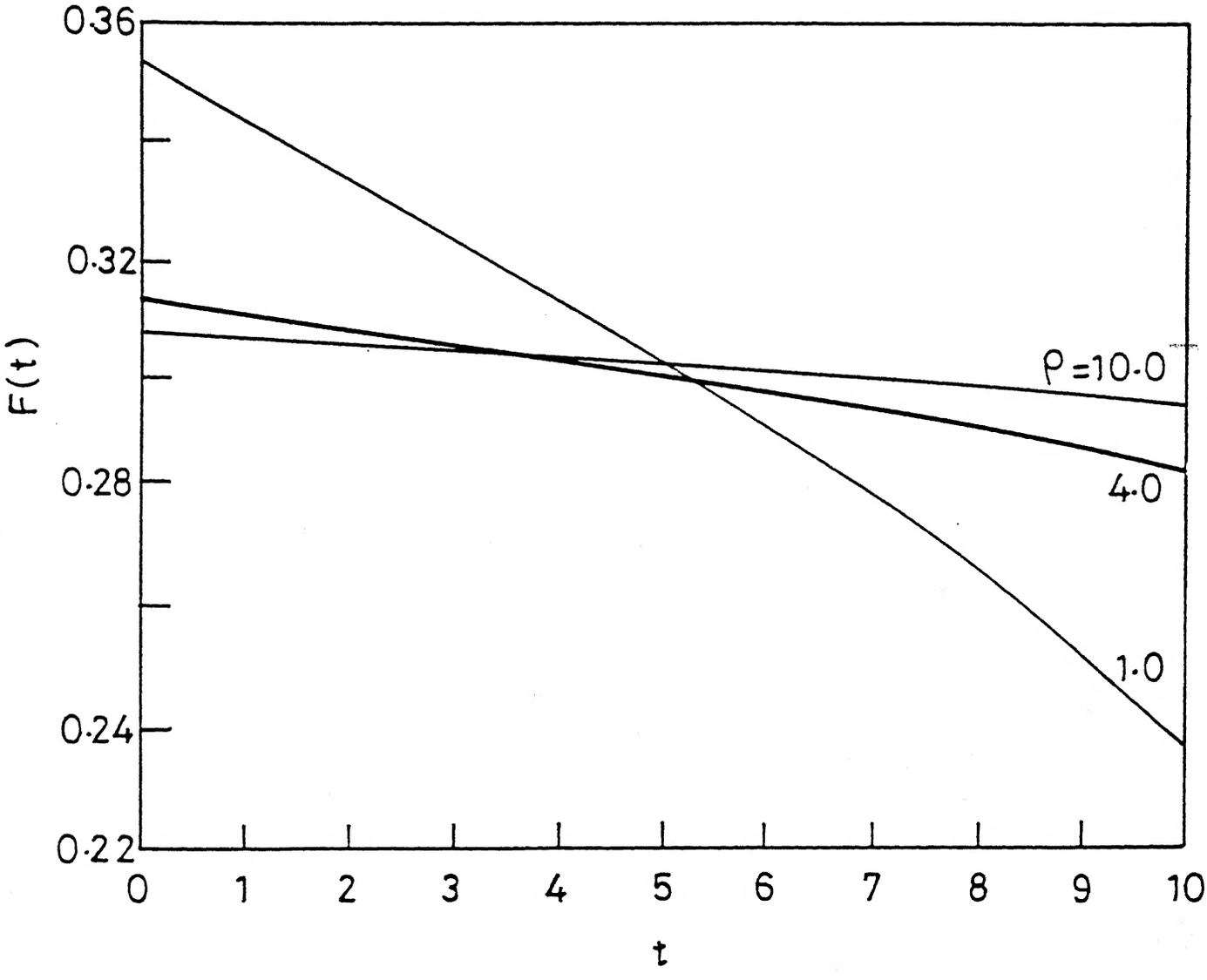

Fig. 3.6: Optimal flow rate profile (fixed final volume, fixed final time). Effect of parameter ρ for a repeated fed-batch biochemical reactor when $S_F < S^*$ (see Table 3.1).

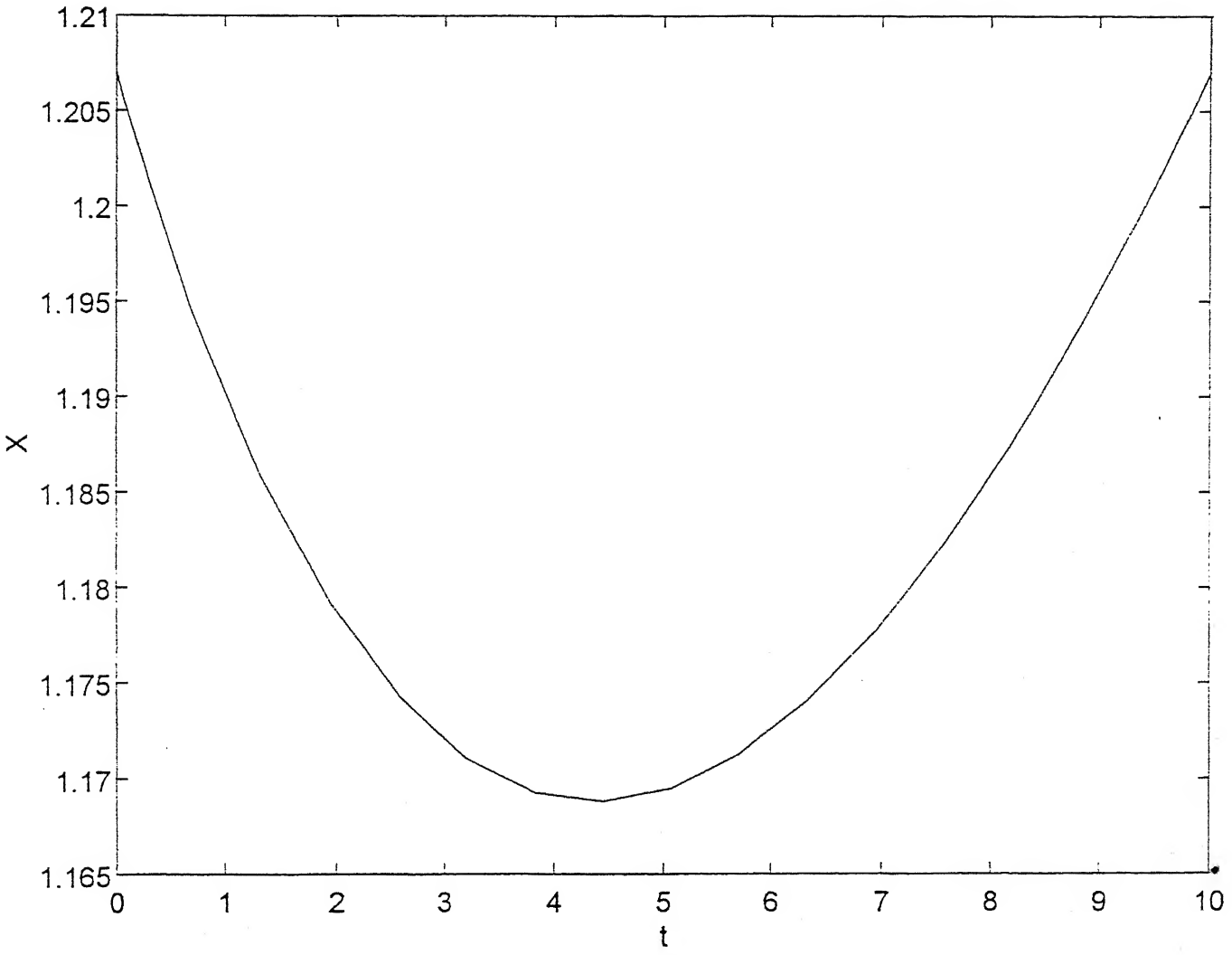

Fig. 3.7: Plot of X vs. time for ρ = 1.0 for optimal profile of Fig. 3.6.

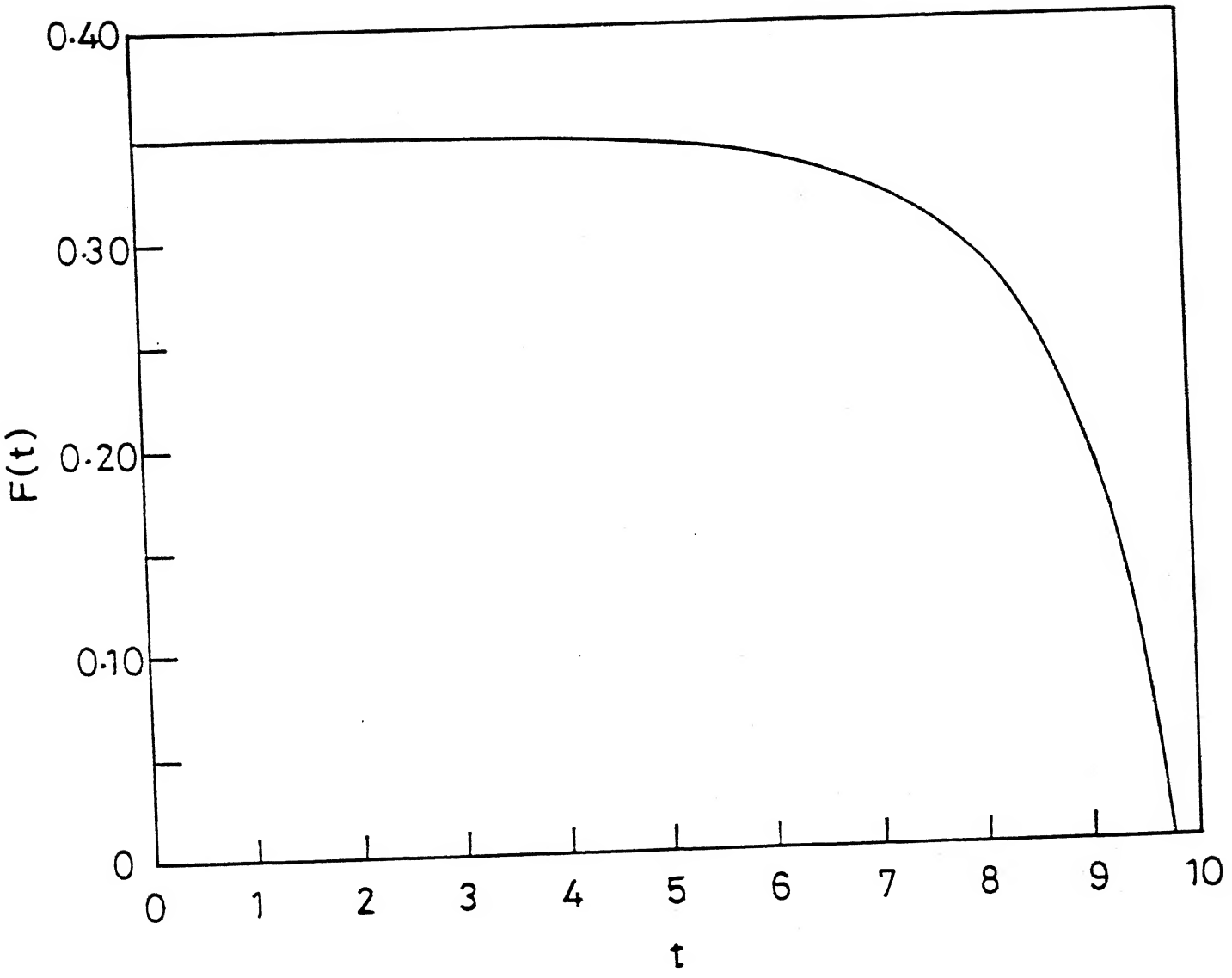

3.8: Plot of flow-rate profile of a fixed final volume, fixed final time for $\rho = 4.0$ when $S_F > S^*$, $r = 0.7$, $S_F = 14.75$

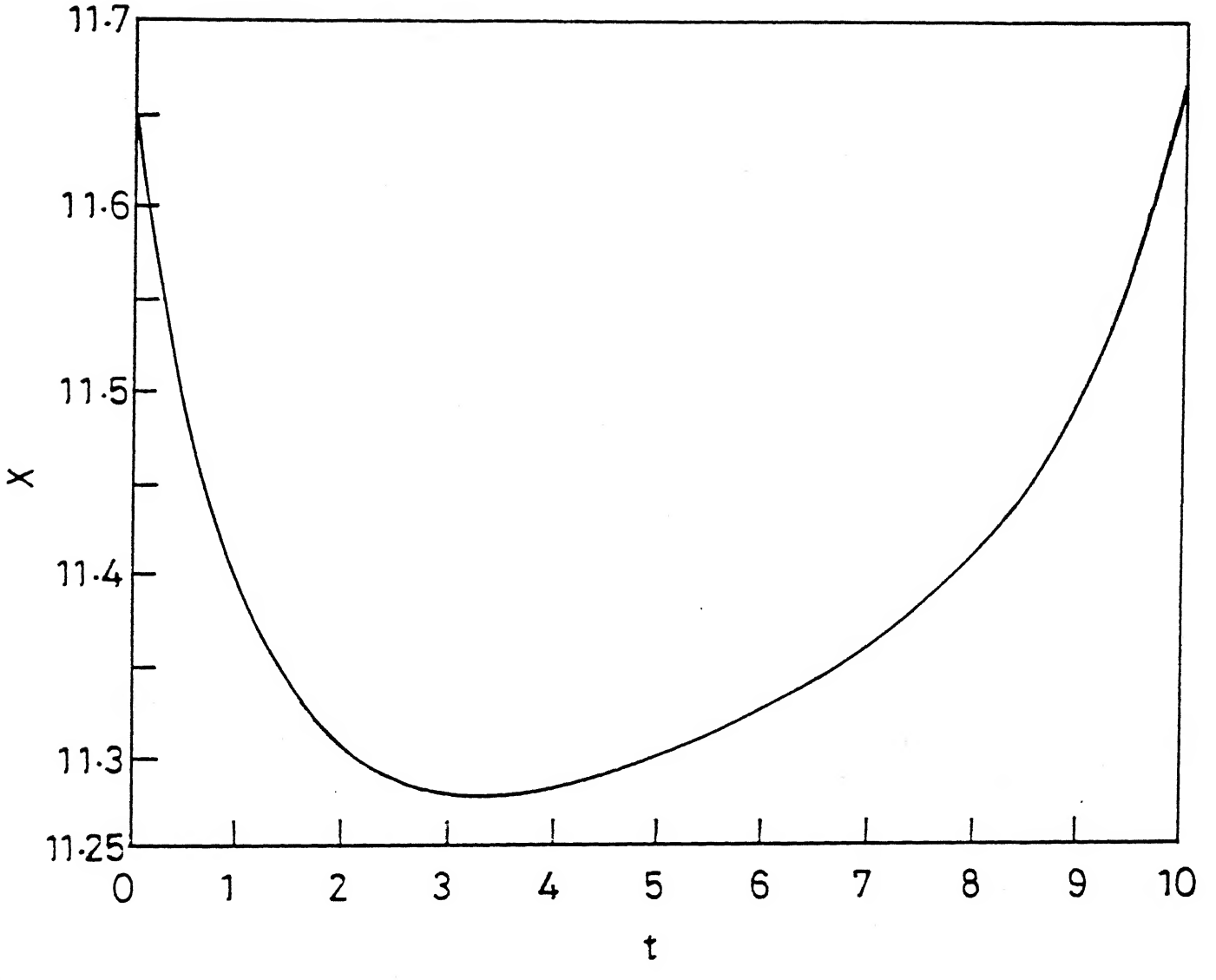

3.9: Plot of X vs. time of a fixed final volume, fixed final time for $\rho = 4.0$ when $S_F > S^*$, $r = 0.7$, $S_F = 14.75$.

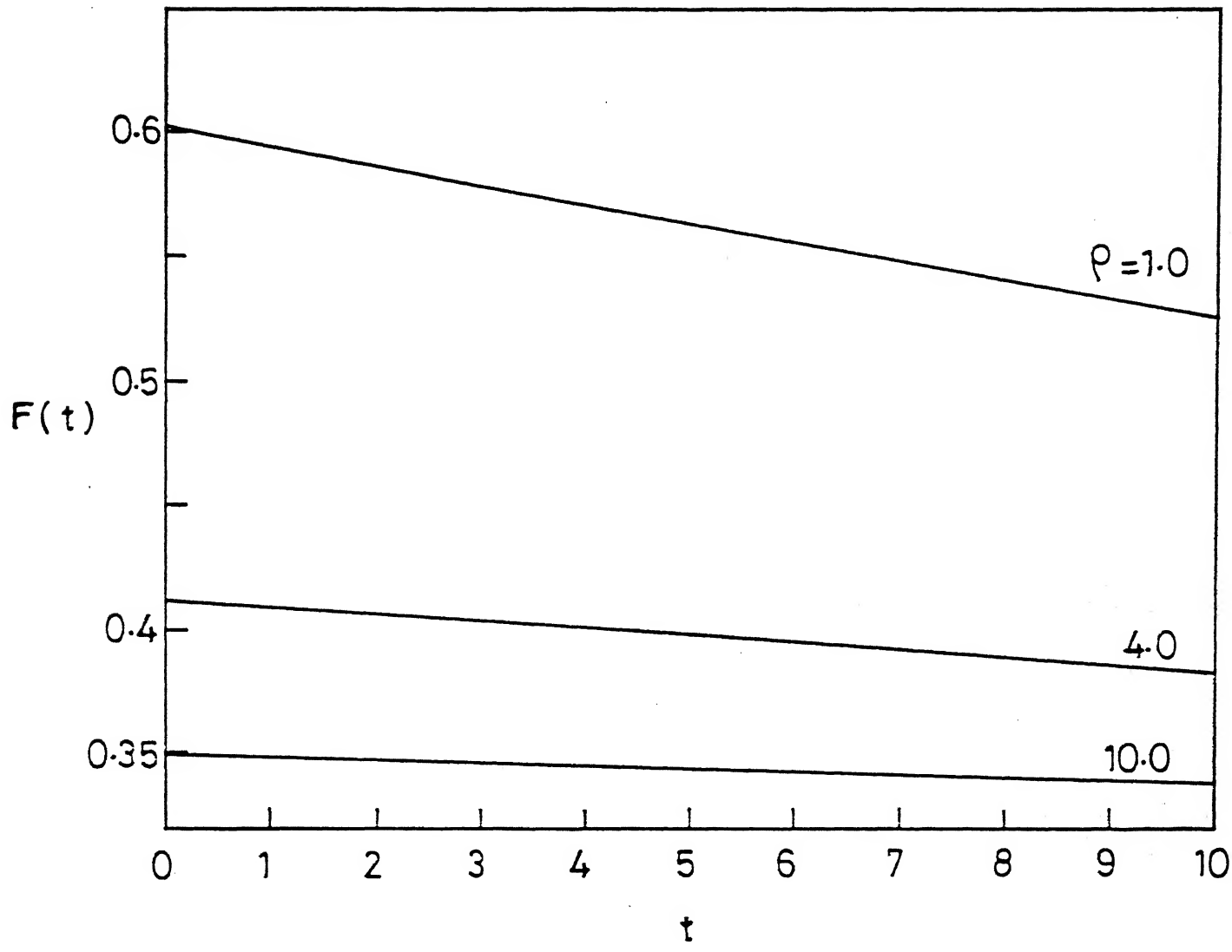

ig. 3.10: Optimal flow rate profile (free final volume, fixed final time). Effect of parameter ρ for a repeated fed-batch biochemical reactor when $S_F < S^*$ (see Table 3.2).

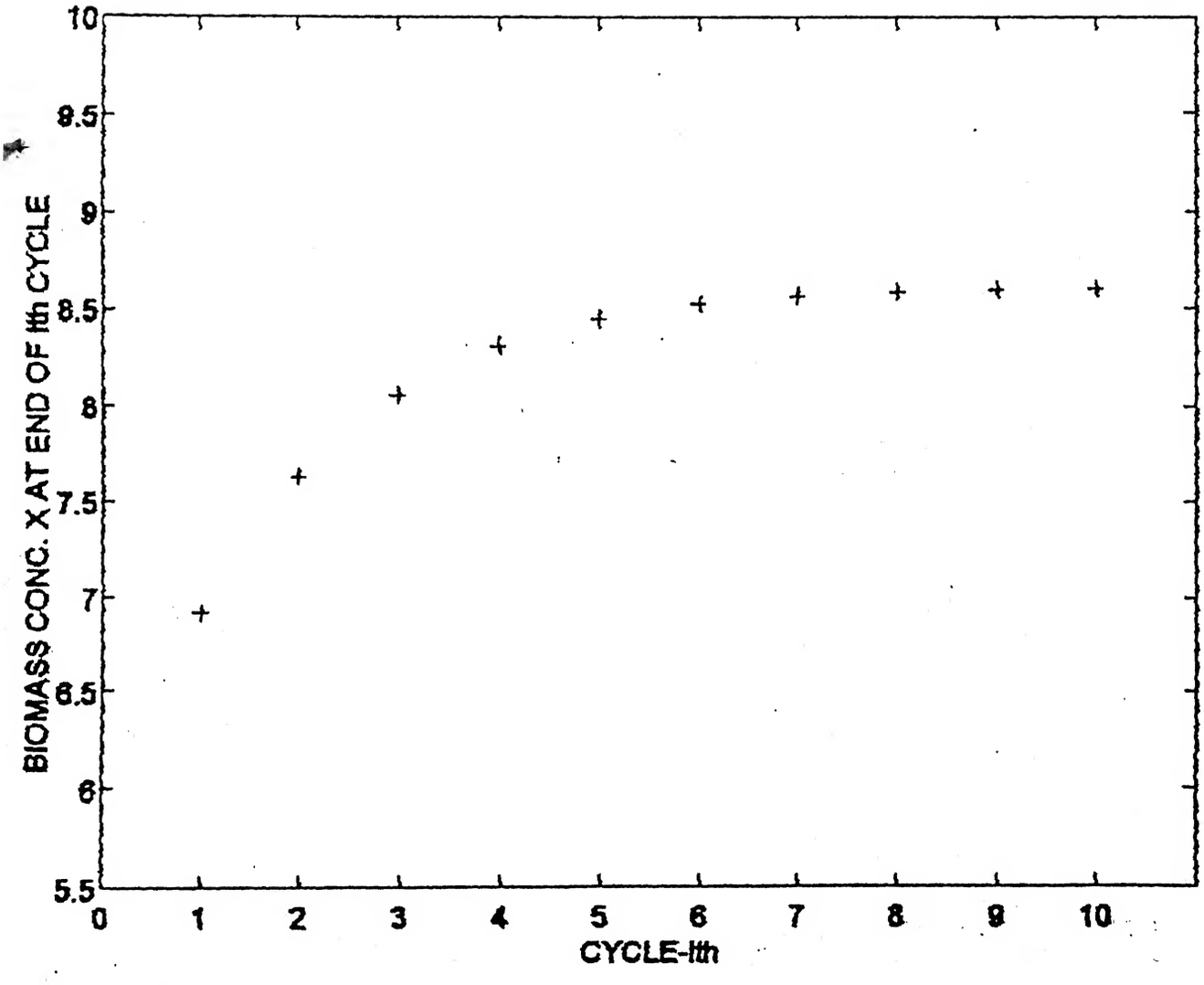

Fig. 4.2 Plot of X versus cycle time for Kc=0.2

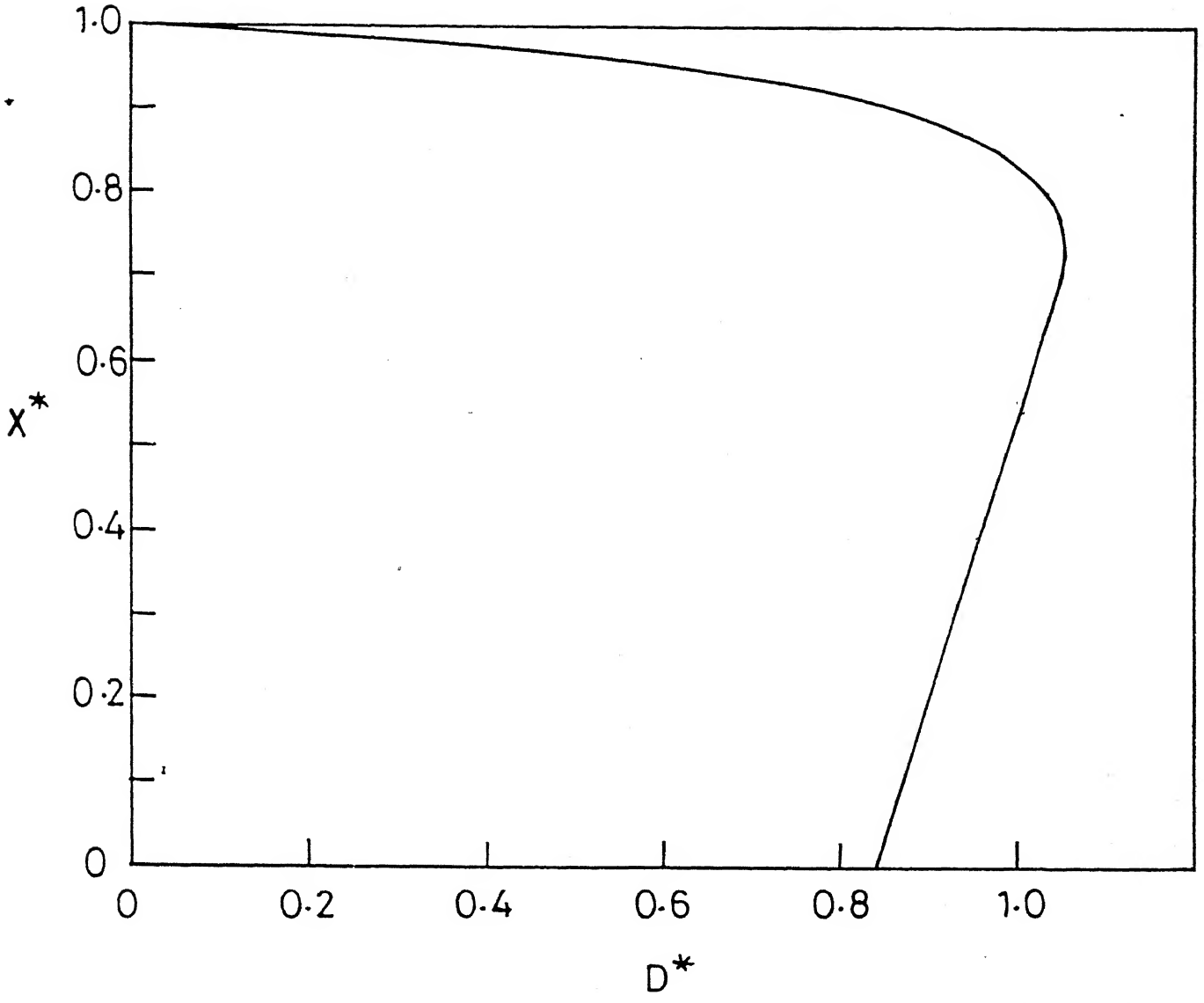

Fig. 4.1 : Bifurcation diagram of a repeated fed batch, constant $\bar{F}$ when S_F = 25.0, r = 0.7.

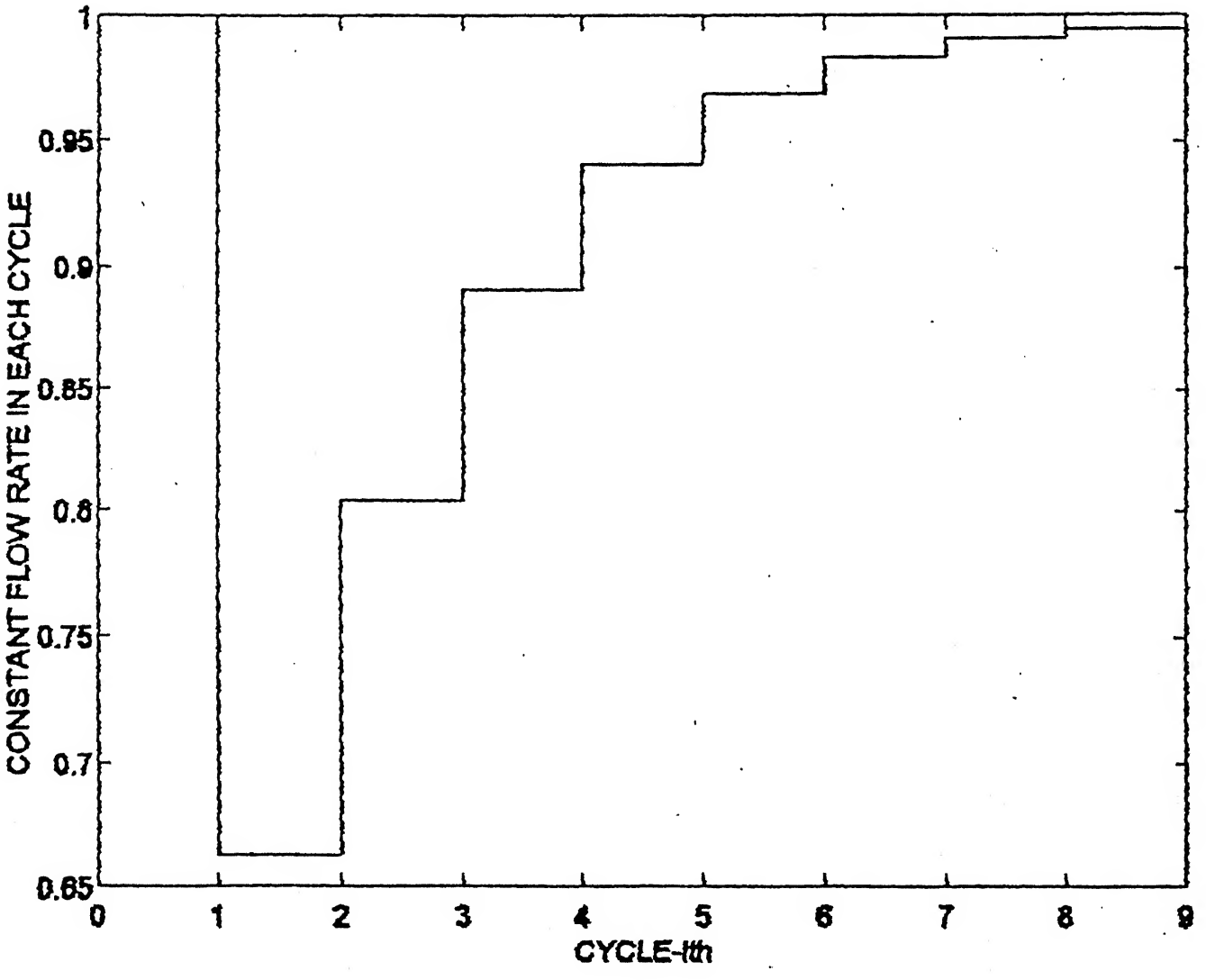

Fig. 4.3 Plot of constant flow rate $\bar{F}$ in each cycle to obtain the set-point X_{sp}= 8.606 for Kc = 0.2.

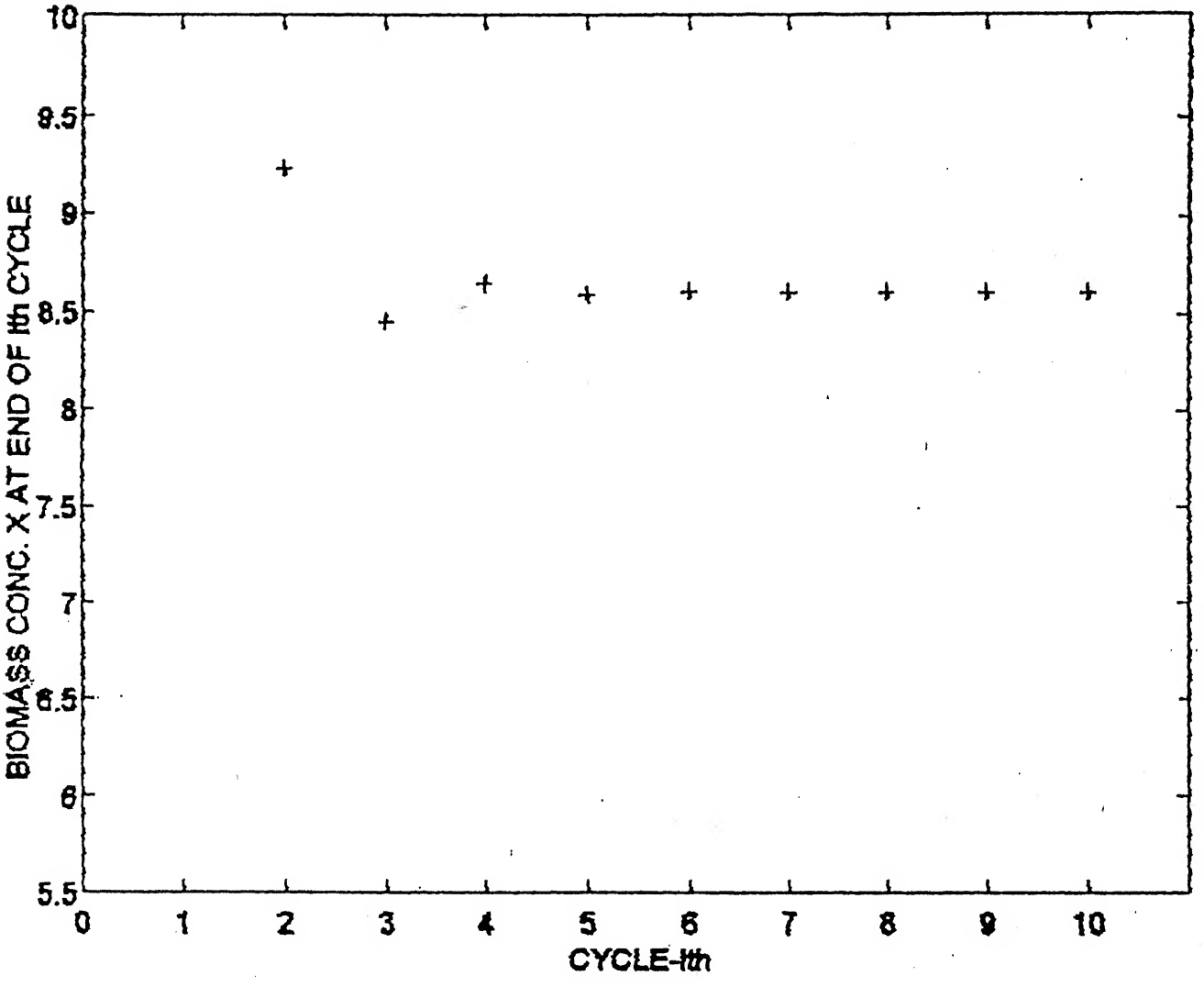

Fig. 4.4 Plot of X versus cycle time for Kc = 0.5

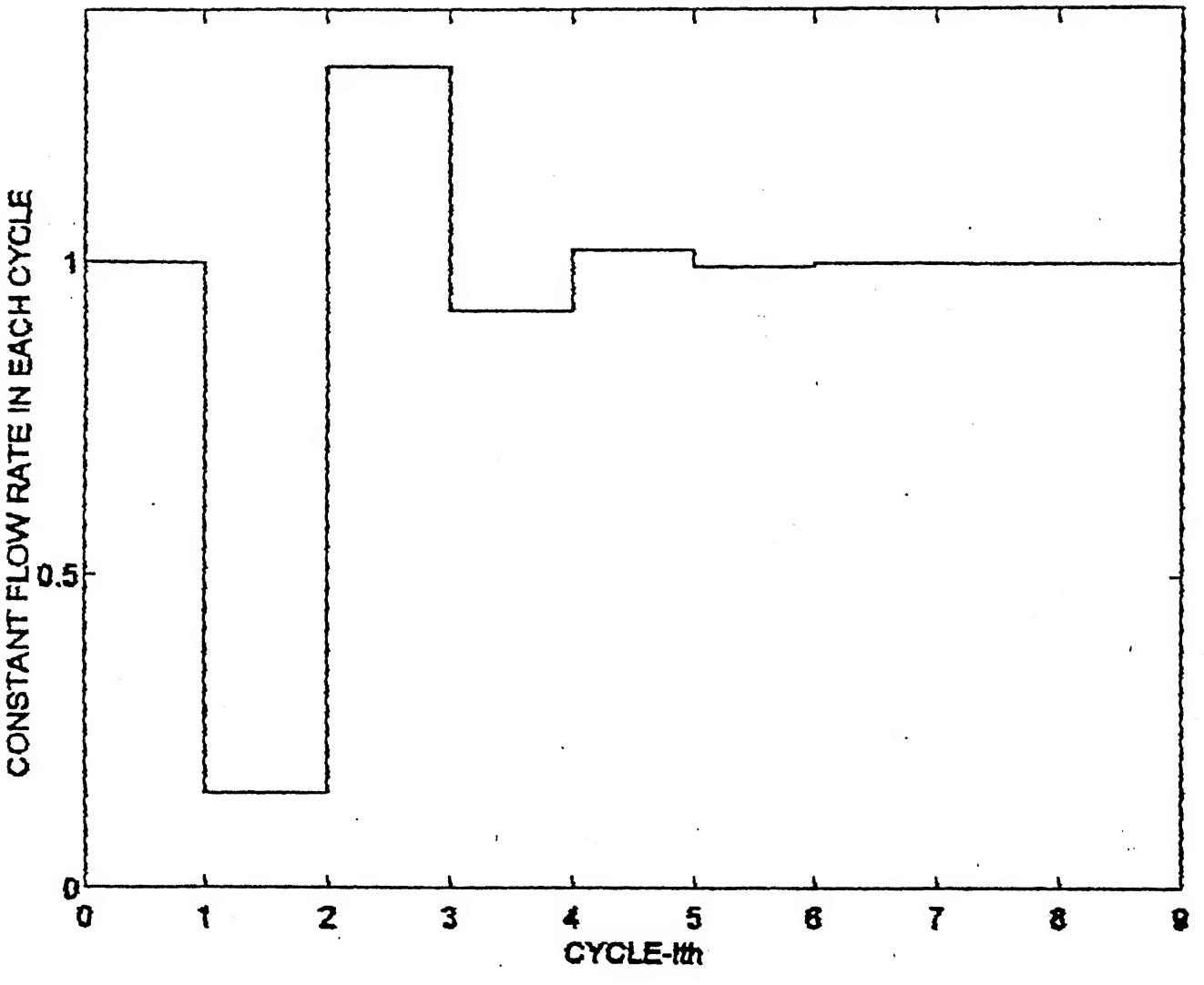

Fig. 4.5 Plot of constant flow rate $\bar{F}$ in each cycle to obtain the set-point X_{sp}= 8.606 for Kc = 0.5.